ELECTRON PARAMAGNETIC RESONANCE STUDIES OF Mn^{2+}, VO^{2+} AND Cr^{3+} IN SINGLE CRYSTALS

By
AZAM ALI ANSARI

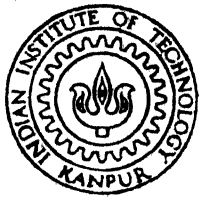

DEPARTMENT OF PHYSICS
INDIAN INSTITUTE OF TECHNOLOGY KANPUR
DECEMBER 1977

ELECTRON PARAMAGNETIC RESONANCE STUDIES OF Mn^{2+}, VO^{2+} AND Cr^{3+} IN SINGLE CRYSTALS

A Thesis Submitted
In Partial Fulfilment of the Requirements
for the Degree of
DOCTOR OF PHILOSOPHY

By
AZAM ALI ANSARI

to the

DEPARTMENT OF PHYSICS
INDIAN INSTITUTE OF TECHNOLOGY KANPUR
DECEMBER 1977

PHY-1977-D-ANS-ELE

Certificate

This is to certify that the work presented in this thesis is the original work of Mr. A.A. Ansari done under our joint supervision, and it is not submitted elsewhere for a degree.

D. Ramachandra Rao
Professor of Physics
I.I.T. Kanpur

Putcha Venkateswarlu
Professor of Physics
I.I.T. Kanpur

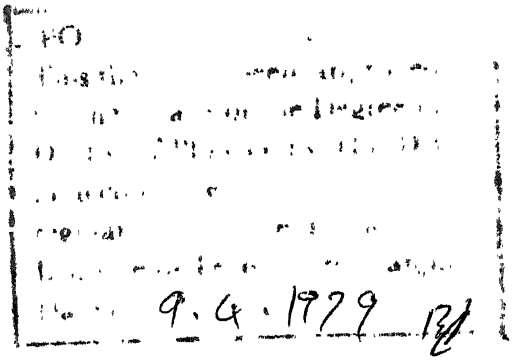

ACKNOWLEDGEMENTS

I take this opportunity to express my gratitude to Professor P. Venkateswarlu for exposing me to the field of spectroscopy, his kind guidance and his interest without which the present work would have been impossible. I am equally grateful to Professor D. Ramachandra Rao for his keen interest and help at various stages of this work. I am highly thankful to Dr. M. D. Sastry for his help in taking EPR spectra and for fruitful discussion.

My thanks are due to Dr. Ramanaiah, Head, Radiochemistry Division, BARC, Bombay who has kindly given permission to use EPR spectrometer of Radiochemistry Division, for this work.

I am thankful to Dr. N. A. Narasimham, Head, Spectroscopy Division, BARC, for getting spectrographic analysis of impurity ions VO^{2+} in the sample KDP:VO^{2+} single crystal system.

I am highly thankful to Professor A. M. Khusro, Vice-Chancellor, Aligarh Muslim University, Aligarh Professor M.Y. Ansari, Principal, Z.H. College of Engg. and Tech., Aligarh Muslim University and Professor T. H. Naqvi, Head, Physics Section of Z. H. College of Engg. and Tech., Aligarh Muslim University for granting me

an extension in the study leave under QIP Programme to about one and a half years.

My sincere thanks are due to Dr. S. D. Pandey, Dr. G. C. Upreti and Dr. U.V. Kumar for fruitful discussion and to Dr. S. C. Sen, and Dr. H. D. Bist for the interest in this work and specific and timely help from Dr. V. K. Jain for help in the final organization of the thesis.

I am thankful to Mr. Nathai Ram Yadav for his help in identifying crystal axes by x-ray technique and to the staff, Physics Workshop, Central Workshop, Glass Blowing, Precision Workshop and electrooptics laboratory for their help.

I can not forget to thank my collegues Dr. K.S. Ramasastry, Dr. Raghubar Dayal, Mr. A.K. Jain, Dr. R.S. Saraswat, Mr. D. Narayana Rao, Mr. Radha Krishna Murthy, Dr. M.S. Ansari, Dr. N.C. Vizia, Dr. Bansi Lal from Physics Department and Mr. S. Barel, Dr. P.N. Shukla, Dr. J.G. Mahanty, Dr. A.N. Singh and others from Chemistry Department for their help and useful discussion.

I thank Miss C. Komala for neat typing of the manuscript and Mr. L. S. Rathaur for running the stencils.

Finally, the financial assistance received from Aligarh Muslim University, Aligarh, Ministry of Education and Social Welfare, Govt. of India, New Delhi and the Indian Institute of Technology Kanpur, is thankfully acknowledged.

CONTENTS

LIST OF TABLES

LIST OF FIGURES

PREFACE

The electron paramagnetic resonance (EPR) technique has proved to be a powerful tool to study the magnetism at microscopic level and yields useful information about the interactions that effect the magnetic state of matter. The site symmetry of impurity ions in the host lattice and its associated lattice defects, symmetry and strength of crystal field at the site of magnetic ion are some of the studies undertaken in solids using EPR techniques. This thesis describes the result of investigations on EPR of $(NH_4)_2C_2O_4.H_2O:Mn^{2+}$, $KH_2PO_4:VO^{2+}$ and $TlAl(SO_4)_2.12H_2O:Cr^{3+}$.

The Chapter 1 deals with a brief introduction to the phenomenon of electron paramagnetic resonance and its application to a variety of physical and chemical problems. Some of the special features of EPR spectra has also been given.

The Chapter 2 describes the basic theory of EPR and other details required for the analysis of the systems studied.

The Chapter 3 describes the EPR study of Mn^{2+} ion in diammonium oxalate monohydrate single crystals. Two magnetically different otherwise, similar centres (related by screw diads) are found corresponding to the ammonium ion sites in the unit cell. The Z-axes of two

centres are found in the ab plane of crystal lattice. The angular separation between two Z-axes is found to be 60^{o}. The EPR study indicates that an Mn^{2+} ion substitutes NH_4^+ ion and gets associated with a vacancy at the first neighbour NH_4^+ ion sites in the ab plane.

The Chapter 4 deals with the EPR study of VO^{2+} ion in the single crystals of potassium dihydrogen orthophosphate. This study revealed the stabilization of two types of vanadium complexes in KH_2PO_4 lattice. The predominant complex, in terms of large intensity, is attributed to VO^{2+} ion entering interstitially and complexing with four oxygens belonging to four neighbouring phosphate groups, to form a nearly square pyramidal complex such as one found in vanadyl acetyl acetone. The absence of any proton structure suggests that the removal of hydrogen cation is the mode of charge compensation. There seems to be magnetically four inequivalent but symmetry related positions for the formation of such a complex. Four pairs of Z-axes of formation of these complexes lie in the ac plane making 20^{o} with c-axis. All these centres become equivalent along c-axis. Apart from this the EPR study reveals the ordered intercrystallization of $[VO(H_2O)_5]^{2+}$ complex in KH_2PO_4 lattice.

The Chapter 5 describes the EPR study of Cr^{3+} doped thallium alum single crystals. The impurity ion seems to have replaced Al^{3+} ions in the host lattice of alum. Four directionally different, otherwise, similar magnetic centres were observed. The crystal field about Cr^{3+} ion in other alkali alums together with the present work indicates that the size of monovalent cations probably affect the atoms at trigonal sites and this seems responsible for the trigonal distortion of crystal field at the Cr^{3+} ion site in the lattice.

CHAPTER I

INTRODUCTION

Electron paramagnetic resonance (EPR) discovered by Zavoisky in 1944, is the phenomenon of resonant absorption of microwave radiation among the Zeeman components of the electronic ground state of a paramagnetic species. This technique gives precise information about the magnetism of the electronic ground state of a system, the only requirement being that the system under study should be paramagnetic. Paramagnetism occurs wherever a system of charges has a resultant non-zero angular momentum. Therefore, when one tries to understand the magnetism of a system at the microscopic level, he ends up with studying the properties of angular momentum, both of spin and orbit, in the electronic ground state. This in turn gives valuable information regarding the way a paramagnetic ion interacts with its surroundings. Transition metal ions and rare earth ions, because of their incomplete d and f electron shells respectively, are good candidates for these studies and have been the subject of a number of very fruitful investigations.

The principle of EPR in its simplest form is as follows. Consider a free atom having orbital and

spin angular momenta $\vec{L}$ and $\vec{S}$ respectively resulting in a total electronic angular momentum $\vec{J} = \vec{L} + \vec{S}$. The magnetic dipole moment associated with the atom is $\vec{\mu} = g\beta\vec{J}$ where β is the Bohr magneton and g is Lande's factor given by the expression

$$g = 1 + \frac{J(J+1)+S(S+1)-L(L+1)}{2J(J+1)}$$

under L-S coupling. In the presence of a magnetic field of strength inadequate to decouple the orbital angular momentum from the spin, the atom may possess any of the discrete set of energies E given by $E = -\vec{\mu}\cdot\vec{H}$

$$\text{or} \quad E = -g\beta M_J H$$

where M_J's are magnetic quantum numbers having integral values from $-J$ to $+J$. The splitting of the energy levels is determined by Lande's g-factor, the separation between two consecutive states being equal to $g\beta H$. If the system is subjected to a microwave radiation field of frequency ν such that $h\nu = g\beta H$, an absorption of energy will take place following the selection rule $\Delta M_J = \pm 1$.

When the paramagnetic ion is doped in a crystal lattice, the paramagnetic resonance spectrum would be different from that of the free ion. In solids,

there are strong interactions between the paramagnetic ion and its immediate diamagnetic neighbours, and the orbital angular momentum gets partially or fully quenched. In such a situation the spectroscopic splitting factor g need not be isotropic. This is because part of the magnetic moment arising from the orbital motion of the electrons is modified by the crystalline electric field and the magnitude of the orbital contribution to the g-value is usually different in different directions and shows an angular variation which follows the symmetry of the crystal field. The total g-value (spin plus orbit) may then be anisotropic by an amount that depends on the magnitude of the orbital contribution to the magnetic moment and on the asymmetry in the crystal field. For all the cases, an anisotropic g-value can be represented by three principal values, g_x, g_y and g_z in a principal axis system i.e., in which $g_{xy} = g_{yz} = g_{zx} = 0$.

In a direction having the direction cosines (ℓ, m, n) with respect to x,y,z axes, the g-value is given by

$$g = (\ell^2 g_x^2 + m^2 g_y^2 + n^2 g_z^2)^{1/2}$$

When once the resonance condition viz., $h\nu = g\beta H$ is achieved there are other factors which control the continuous absorption of energy by the magnetic system. The population in the Zeeman components obeys Boltzmann distribution, and at any given temperature the lower level will be more populated than the upper one. When the resonance absorption occurs there will be a tendency to equalise the populations, and unless there are mechanisms which maintain the population difference continuously, paramagnetic resonance absorption ceases to be significant. Such mechanisms are called relaxation processes in which lattice plays a significant role. It acts like a huge reservoir with which the magnetic system changes energy with a characteristic time, usually represented as T_1, called Spin-Lattice relaxation time. This is a characteristic of a given magnetic ion in a lattice at a particular temperature and normally it increases with decrease of temperature.

The spin-lattice relaxation time contributes to the width of an EPR line. Another frequent case of line broadening occurs due to high concentration of paramagnetic ions in solids. This arises due to dipole-dipole interaction and it can be considerably reduced by diluting a paramagnetic salt with an isomorphic diamagnetic substance.

EXPERIMENTAL OBSERVATION OF EPR

The manifestation of magnetic resonance absorption is normally observed by detecting the magnetization of the spin system due to the alternating magnetic field $H_1(t)$. There will be two components of that magnetization, usually represented by the corresponding susceptibility χ , one in phase with $H_1(t)$: χ' , and the other 90° out of phase with $H_1(t)$: χ'', χ' and χ'' are related by Kramers-Kronig equations and they give dispersion and absorption of energy by the spin-system respectively. The experimentally observed quantity in the absorption mode is $d\chi''/dH$ as a function of H. In the present investigations, a Varian EPR spectrometer V-4502, operating at X-band frequencies (9-10 GHz) has been used.

SPECIAL FEATURES OF EPR SPECTRA

a. Fine Structure

In paramagnetic systems, which form part of a solid or a complex, where the ground state is an orbital singlet with spin multiplicity greater than two (i.e., $S \geq 1$) very often there are initial splittings of the ground state multiplet even in the absence of magnetic field. The most important cause of these splittings is the Stark effect resulting from asymmetrical crystalline fields together with the spin-orbit interaction which mixes the

ground state with the excited state. Whenever, there are zero field splittings of the ground state multiplet, the Zeeman components cease to be equally spaced and all the resonant transition ($\Delta M_s = \pm 1$) do not occur at the same energy and there will be 2S well separated transitions. This is called the 'fine structure' of the paramagnetic resonance spectrum. The fine structure separations give valuable quantitative information about the crystal field interactions and will be discussed in detail in the next chapter.

b. Hyperfine Structure

Whenever the nucleus of a paramagnetic ion has spin I, there will be a magnetic interaction of the type $\vec{I}.\underline{A}.\vec{S}$ between the electron and the nucleus and each fine structure energy level splits into $(2I + 1)$ levels. The r.f. field which causes electronic 'spin-flip' does not cause simultaneous nuclear spin transitions in the first order. The selection rules therefore are

$$\Delta M_s = \pm 1, \qquad \Delta m_I = 0$$

c. Super-Hyperfine Structure

This results from hyperfine interaction between the metal electron and the neighbouring ligands and nuclei. This gives quantitative information about

the delocalization of electron over the ligands. This is among the most elegant contributions of EPR towards understanding the nature of chemical bond.

Over the last two decades, EPR has been most successfully used for a variety of problems in physics and chemistry evolving from technique-oriented to problem-oriented research. EPR together with optical and thermal studies contributed substantially towards a clearer understanding of formation and structure of colour centres in solids. Its most recent contribution to the medical sciences is the identification of a malignant tumour which may at a future date, lead to a clearer understanding of the cause of cancer. A electron paramagnetic resonance of 3d transition metal ions has been quite well understood and therefore these ions serve as excellent candidates to probe the crystal fields. Among 3d transition ions $V^{4+}(3d^1)$, $Cr^{3+}(3d^3)$, $Mn^{2+}(3d^5)$ and $Cu^{2+}(3d^9)$ can be most effectively used as their EPR can be observed over a wide temperature range including room temperature. The present study deals with the study of KH_2PO_4 using VO^{2+} as probe, $(NH_4)_2C_2O_4 \cdot H_2O$ using Mn^{2+} as a probe and $TlAl(SO_4)_2 \cdot 12H_2O$ using Cr^{3+} as a probe. The study on $VO^{2+}:KH_2PO_4$ revealed for the first time about the functioning of KH_2PO_4 lattice in helping the stablization of certain VO^{2+}

complexes. The work on $(NH_4)_2\ C_2O_4 \cdot H_2O$ is the first investigation of this lattice using paramagnetic ions a probes. The work on Cr^{3+}:$NH_4Al(SO_4)_2 \cdot 12H_2O$ has been taken up as a part of the work done earlier in this laboratory to understand the effect of transition impurities on the different structural modification of alums.

Further details regarding the subject can be obtained from a list of general references given at the end of this chapter.

GENERAL REFERENCES

1. W. Low, Paramagnetic Resonance in Solids, (Academic Press New York and London, 1960).

2. S. A. Al'tshuler and B. M. Kozyrev, Electron Paramagnetic Resonance, (Academic Press, New York and London, 1964).

3. Raymond S. Alger, LPR Techniques and Applications, (Interscience Publications, a Division of John Wiley and Sons, 1968).

4. W. Gordy, W. V. Smith and R. F. Trambarulo, Microwave Spectroscopy, (John Wiley and Sons, New York and London, 1953).

5. P. B. Ayscough, Electron Spin Resonance in Chemistry, (Mathuen and Co., Ltd., London EC4, 1967).

6. K. D. Bowers and J. Owen, Reports on Progress in Physics 13, 304, (1955).

7. A. Abragam, B. Bleaney, Electron Paramagnetic Resonance of Transition Ions, (Clarendon Press Oxford, 1970).

8. G. E. Pake, Paramagnetic Resonance, (W. E. Benjamin, Inc New York, 1962).

9. Carl J. Ballhausen, Introduction to Ligand Field Theory, (Mcgraw hill, 1962).

10. J. W. Orton, Electron Paramagnetic Resonance (Iliffe Books Ltd., London 1968).

11. T. M. Dunn, D. S. McClure and R. G. Pearson, Some Aspect of Crystal Field Theory (Harper and Row, Publishers, Incorporated 1965).

12. M. T. Hutchings, Solid State Physics Vol. 16 in F. Seitz and D. Turnbull edition.

CHAPTER 2

THEORY

ABSTRACT

General Hamiltonian for a paramagnetic ion in a crystalline field is described. Crystal-field splitting of the ground state of the paramagnetic ion has been elaborated taking the example of Cr^{3+} ion in a crystalline field of octahedral symmetry. The effect of spin-orbit coupling on the g-factor is described. A short description of the spin Hamiltonian is given. A brief summary of the mechanism of zero field splitting of an S-state ion in the host lattice is described. An anomalous hyperfine splitting of S-state ion is explained.

The Hamiltonian for a paramagnetic ion in a solid may be expressed[1] as

$$\mathcal{H} = H_E + H_{LS} + H_{SI} + H_Q + H_V + H_{SH} + H_{IH} \qquad (2.1)$$

The terms occuring in the above expression have the following meanings.

1. H_E stands for the sum total of the kinetic energy of electrons, their potential energy in the nuclear field and electrostatic potential energy due to electron repulsion. Mathematically it can be expressed as below:

$$H_E = \sum_i \left(\frac{p_i^2}{2m} - \frac{Ze^2}{r_i}\right) + \sum_{i \neq j} \frac{e^2}{r_{ij}} \qquad (2.2)$$

Here p_i represents the magnitude of linear momentum of ith electron of mass m and charge e, r_i, the distance of the electron i from the nucleus of atomic number Z, and r_{ij}, the distance between electrons i and j. The contribution to the energy from this term is of the order of 10^5 cm^{-1}.

2. The term H_{LS} gives the spin-orbit coupling and it can be written as

$$H_{LS} = \sum_{i,j} \lambda_{i,j} \ell_i s_j \qquad (2.3)$$

where ℓ_i and s_j represent orbital and spin angular momenta of electron i and electron j respectively. The above expression can, however, be expressed in a simple form

$$H_{LS} = \lambda \vec{L} \cdot \vec{S} \quad \text{where } L = \sum_i \ell_i$$

and $S = \sum_j s_j$, of free ion so long as we consider only terms derived form the ground state defined by equation (2.2). The interaction energy is generally of the order of 10^2 to 10^3 cm^{-1}.

3. H_{SI} represents the interaction of electronic spin (S) and nuclear spin (I) which can be expressed as $\vec{S} \cdot \underline{A} \cdot \vec{I}$. The tensor $\underline{A}$, known as hyperfine interaction tensor, may be isotropic or anisotropic. The isotropic hyperfine interaction is attributed to Fermi contact which has non-vanishing contribution for electronic wave function having a finite value at the nucleus. The expression of this interaction is given by

$$\frac{8\pi}{3} g_N \beta_N g \beta \, |\psi(0)|^2,$$

where $\psi(0)$ is the wave function at the nucleus and suffix N refers to the nucleus. The anisotropic contribution to the hyperfine interaction arises due to spin-spin interaction. If μ_N and μ_e represent the magnetic

dipole moments corresponding to the nuclear and electronic angular momenta respectively, the classical expression for the dipole interaction energy is given by

$$V_N = \frac{\vec{\mu}_e \cdot \vec{\mu}_I}{r^3} - \frac{3(\vec{\mu}_e \cdot \vec{r})\ (\vec{\mu}_I \cdot \vec{r})}{r^5} \qquad (2.4)$$

For a quantum mechanical system, the magnetic moment must be replaced by the corresponding operator. Thus

$$H_{dip} = -g_e g_N \beta_N \left[\frac{\vec{S} \cdot \vec{I}}{r^3} - \frac{3(\vec{S} \cdot \vec{r})(\vec{I} \cdot \vec{r})}{r^5} \right] \qquad (2.5)$$

The total hyperfine interaction energy (isotropic and anisotropic) can be written as $\vec{S} \cdot \underset{\sim}{A} \cdot \vec{I}$ where $\underset{\sim}{A} = A_0 \underset{\sim}{1} + A'$, where $\underset{\sim}{1}$ is the unit tensor. This interaction gives rise to hyperfine levels. The separation of hyperfine levels is of the order of 10^{-2} cm^{-1}.

4. H_Q stands for nuclear quadrupole interaction and it can be written as $\vec{I} \cdot \underset{\sim}{Q} \cdot \vec{I}$. The components of quadrupole tensor Q_{ij} are proportional to second order derivative components $V_{ij} = \partial^2 V / x_i x_j$ of electrostatic potential V. In the principal axis system Q'' may be expressed as

$$\underset{\sim}{Q} = \frac{eQ}{2I(I-1)} \begin{bmatrix} V_{xx} & 0 & \\ & V_{yy} & \\ 0 & & V_{zz} \end{bmatrix} \qquad (2.6)$$

The quadrupole interaction energy for axial symmetry is given by

$$\vec{I}.\underset{\sim}{Q}.\vec{I} = \frac{eQV_{zz}}{4I(I-1)} [3M_I^2 - I(I+1)] \qquad (2.7)$$

This interaction term shifts the hyperfine level by a small amount 10^{-4} cm^{-1}.

5. H_V term describes the crystal field interaction and may be represented by

$$H_V = \sum_i e_i V(r_i) \qquad (2.8)$$

where $V(r_i)$ is the crystal field potential at the location of electron i.

6. The last two terms in the Hamiltonian represent the electron-Zeeman and nuclear-Zeeman interaction terms and may be written as

$$H_{SH} = \beta(\vec{L} + g_e\vec{S}).\vec{H} \qquad (2.9)$$

and

$$H_{IH} = (h/2\pi) \sum_i - \gamma_i \vec{I}_i.\vec{H} \qquad (2.10)$$

where γ_i is the magnetogyric ratio of the ith nucleus. The contribution of latter term is negligible ($10^{-4}cm^{-1}$).

In order to know the exact solution of the general Hamiltonian, one should solve the Schrodinger equation. But because it poses a formidable mathematical difficulty to do that, the solutions are obtained by using the perturbation theory. Since the effect of crystal field on the state of transition metal ions of iron group is very large, it is dealt with separately.

CRYSTAL FIELD SPLITTING

The magnetic ion in a crystalline solid is subjected to a stark field. This field is due to electronic and nuclei charges of neighbouring ions. In the crystal field approximation, the sources of stark field are regarded as point charges or dipoles located at the centres of corresponding charges (ligands). These surrounding ions have some symmetry about the metal ion. Depending on the symmetry of the field, the degeneracy of ground state of the magnetic ions is lifted completely or partly. The symmetry considerations have led Bethe[2] to find a qualitative solutions for the splitting of degenerate electronic states with the help of group theory. How the symmetry of crystalline field removes the degeneracy of on electronic state can, however, be visualized in the following manner.

Let us consider, for example, an electron of a paramagnetic ion in its 'd' orbital. Let the ion be located in an octahedral crystalline field, obtained by a set of six equal and identical point charges situated at equal distances on X, Y, and Z-axes of a Cartesian coordinate system from its origin where the seat of paramagnetic ion is taken. Out of the five d orbitals d_{xy}, d_{yz} and d_{xz} are located in similar environments of crystal field and therefore correspond to equal energy. The orbital $d_{x^2-y^2}$ with its area of maximum charge density lying nearest to the charges on X and Y- axes corresponds to higher electrostatic energy as compared to d_{xy}, d_{yz} and d_{xz} orbital. Similarly the energy of d_{z^2} orbital is greater than that of d_{xy}, d_{yz}, or d_{xz} The energy of $d_{x^2-y^2}$ and d_{z^2} orbitals comes out to be same though it is not so apparent here. Therefore it is seen from the symmetry consideration that the degeneracy of d-orbital electron in a crystalline field of octahedral symmetry is partly lifted. We get a low lying triplet state and a higher lying doubly degenerate state.

The degeneracy of the ground level can also be lifted due to Jahn Teller effect. This states that a non-linear molecule with the degenerate ground state is unstable and it distorts in such a way that the ground state becomes non-degenerate.

There is another important theorem which deals with the restriction on degeneracy which can be removed by an electrostatic field. This is known as Kramers Theorem. This states that the degeneracy of any level of a system with an odd number of electrons cannot be reduced below two-fold by a purely electrostatic field. The degeneracy of such a system can only be removed by a magnetic field. For the understanding of crystal field splitting quantitatively, let us consider a paramagnetic ion situated at r near the origin of a coordinate system. Let the radius vector R_j represents the location of a discrete point charge q_j constituting the ligands. The potential due to point charge q_j at the position occupied by a magnetic ion is given by

$$V_j = \frac{q_j}{|\vec{R}_j - \vec{r}|} \tag{2.11}$$

The potential due to all the surrounding ligands will therefore be

$$V = \sum_j V_j = \sum_j \frac{q_j}{|\vec{R}_j - \vec{r}|} \tag{2.12}$$

where the index j sums over all the surrounding ligands. Sometimes it is convenient to express the potential in rectangular coordinates. For example, when the symmetry

of the crystalline field is octahedral the potential at a point having coordinates (x, y, z) due to negative points charges q's located at distance ± d from the origin on X, Y and Z-axes is given[3] by

$$V(x,y,z) = 6q/d + (35q/4d^5)\ [x^4+y^4+z^4 -(3/5)r^4] \qquad (2.13)$$

Here the series is terminated at terms containing only the fourth power of r, as contribution from higher order terms would be zero for 'd' electron with which the work in this thesis is concerned.

If the charges located on Z-axis are slightly displaced away from the origin by a distance ε as in Fig. 2.1, the symmetry of crystalline field becomes tetragonal. Now the potential due to this is given[3] by

$$V_t(x,y,z) = A_t[(3z^2-r^2)+(1/d^2)(35z^4/3 - 10r^2z^2+ r^4)] + B_c[x^4+y^4+z^4- (3/5)r^4] \qquad (2.14)$$

where $A_t = -3q\varepsilon/4$ and $B_c = 35q/4d^5$. It is assumed that $\varepsilon \ll d$. Here the co-efficient A_t gives the amount of tetragonal distortion present on the octohedral field.

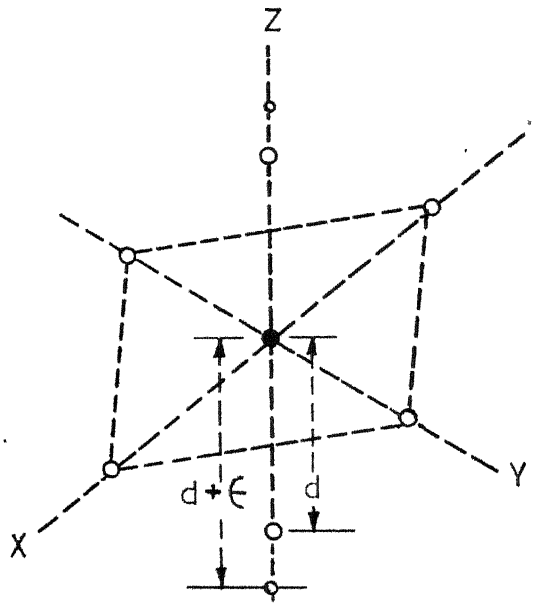

Fig.2.1 Schematic representation of a paramagnetic ion located at octahedral/tetragonally disorted octahedral site.

● ---- Paramagnetic ion

o ---- Ligand ions constituting octahedron

∘ ---- Displaced position of ligand ion on Z-axis

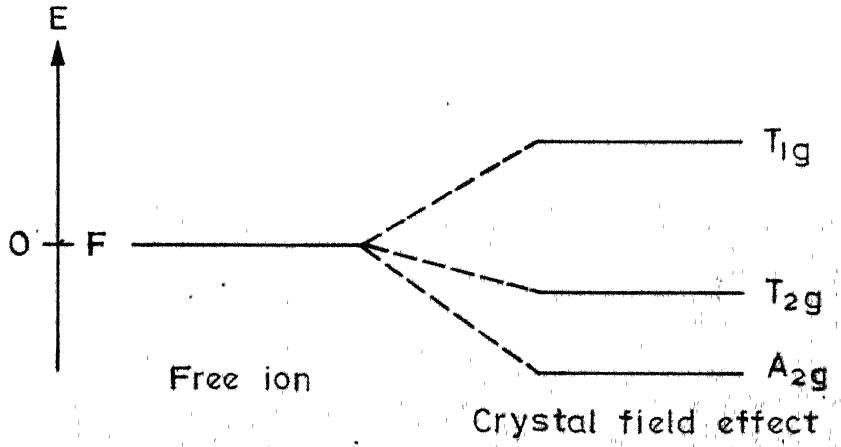

Fig.2.2 Schematic representation of energy levels of an F-state ion in octahedral crystal field.

The modification in the energy of d-electrons produced by the crystal field can be computed by matrix elements of the type $J, M_z \; H_V \; J, M_z$. In this expression H_V represents potential energy operator and J, M_j refer to total angular momentum and its projection on the quantization axis. For the purpose of computing the contribution of crystal field to energy, the function x, y and z in the crystal field operator may be replaced by the angular momentum operators J_x, J_y and J_z, based on Stevenson Theorem which states that for a set of eigen functions of J^2 and J_z all having the same eigen value J, the matrix element of x and J_x, y and J_y and z and J_z are respectively proportional to one another.

In the transformation noncommuting property of the operators is to taken into account. The operator equivalents of some functions are given in the table below[3]

Function	Operator Equivalents
x^n, y^n, z^n	$(j_x)^n, (j_y)^n, (j_z)^n$
r^2	$J(J+1)$
x^2z^2	$(1/6)[3J_x^2 j_z^2 + 3J_z^2 J_x^2 - 2J_x^2 + 3J_y^2 - 2j_z^2]$
r^4	$J^2(J+1)^2 - (1/3)\, J(J+1)$

The operator equivalent of β_c $(x^4 + y^4 + z^4 - (3/5)\, r^4)$ is thus

$$\frac{\beta_c}{20}\left[35J_z^4 - 30J(J+1)J_z^2 + 25J_z^2 - 6J(J+1) + 3J^2(J+1)^2\right] + \frac{\beta_c}{8}\left(J_+^4 + J_-^4\right) \tag{2.15}$$

and the operator equivalent for $A_t\,(3z^2 - r^2)$ is

$$\alpha_t\left[3J_z^2 - J(J+1)\right] \tag{2.16}$$

where β_c ; α_t are constants. The above expressions are true for weak field case. For ions in the crystal field of intermediate strength J's are replaced by L's. Thus,

$$H_{oct} = \frac{\beta_c}{20}\left[35L_z^4 - 30L(L+1)L_z^2 + 25L_z^2 - 6L(L+1) + 3L^2(L+1)^2\right] + \frac{\beta_c}{8}\left(L_+^4 + L_-^4\right) \tag{2.17}$$

$$H_{tet} = H_{oct} + \alpha_t\left[3L_z^2 - L(L+1)\right] \tag{2.18}$$

The matrix elements of an F-state ion in a crystalline field of octahedral symmetry are given below[3]:

	|3>	|2>	|1>	|0>	|-1>	|-2>	|-3>
|3>	$(3/10)\Delta$				$(\sqrt{15}/10)\Delta$		
|2>		$(-7/10)\Delta$				$\Delta/2$	
|1>			$\Delta/10$				$(\sqrt{15}/10)\Delta$
|0>				$3\Delta/5$			
|-1>	$(\sqrt{15}/10)\Delta$				$\Delta/10$		
|-2>		$\Delta/2$				$(-7/10)\Delta$	
|-3>			$(\sqrt{15}/10)\Delta$				$(3/10)\Delta$

The secular determinant can be arranged into diagonal blocks, which on diagonalization separately give

$W(T_{1g}) = (3/5)\Delta$ (Triply degenerate)

$W(T_{2g}) = (-1/5)\Delta$ (Triply degenerate)

$W(A_{2g}) = (-6/5)\Delta$ (Singlet)

Here $\Delta = 30\beta_c$, and T_{1g}, T_{2g} and A_{2g} denotes the species the levels belongs to, under the octahedral symmetry group. This splitting is shown in Fig. 2.2.

SPIN-ORBIT COUPLING

The effect of crystalline field is to remove partly or completely the orbital degeneracy of the ground state of a magnetic ion. When the orbital degeneracy is lifted completely, the orbital angular momentum of the ion is said to be quenched. This tendency of crystal field is is opposed by spin-orbit couplin which interacting with some of the excited states, tries to mix some orbital angular momenta to the ground state. The amount of admixture of a state into the ground state, however, depends inversely upon its separation from the ground state level. The result of this admixture is to deviate the value of effective 'g' factor from that of the free spin of electron. The Hamiltonian for a free atom having spin-orbit interaction and subjected to a magnetic field H is given[3] by

$$H' = H_{mag} + H_{SO} = \beta H (\vec{L} + g_e \vec{S}) - \vec{L}.\vec{S} \qquad (2.19)$$

The terms in the above expression stand for their usual meaning and g_e represents g factor for electronic spin. Now if we assume the ground state to be nondegenerate orbitally and denote it by $|G, M_s\rangle$ in the first order approximation, the energy of ground state is given[3] by the diagonal term and is therefore

$$E_G^{(1)} = \langle G, M_s | \beta H_z (L_z + g S_z) + \lambda (\vec{L} \cdot \vec{S}) | G, M_s \rangle \qquad (2.20)$$

where the quantization axis is taken as the z axis. Rearranging, we have

$$E_G^{(1)} = \langle G, M_s | \beta H_z g_e S_z | G, M_s \rangle + \langle G, M_s |$$

$$| (\beta H_z + \lambda S_z) L_z | G, M_s \rangle$$

The first term in equation (2.20) is the spin only Zeeman energy. The second term in this equation, can be written[3] as

$$\langle M_s | (\beta H_z + \lambda S_z) | M_z \rangle \quad \langle G | L_z | G \rangle$$

Since the expectation value of L_z is zero this term vanishes.

The second order contribution[3] in the Hamiltonian matrix is

$$H'_{M_s, M'_s} = - \Sigma' \frac{| \langle G, M_s | (\vec{\beta H} + \vec{S}) \cdot \vec{L} + g_e \vec{\beta H} \cdot \vec{S} | n, M'_s \rangle |^2}{E_n^{(0)} - E_G^{(0)}} \qquad (2.21)$$

Here Σ' implies summation over all values of n [illegible] excepting n = G.

The matrix element from the second term in equation (2.21) will be zero since $\langle G | n \rangle = 0$ while the first term yields

$$H'_{M_s, M'_s} = -\sum_n{}' \left[\frac{\langle M_s | (\beta\vec{H} + \vec{S}) \cdot \langle G | \vec{L} | n \rangle \langle n | \vec{L} | G \rangle}{E_n(0) - E_G(0)} \cdot \right. \\ \left. \cdot (\beta\vec{H} + \vec{S}) M'_s \right] \qquad (2.22)$$

Since the outer product of two matrix elements yields a second rank tensor, we can define

$$\Lambda_{ij} = -\sum_n{}' \frac{\langle G | L_i | n \rangle \langle n | L_j | G \rangle}{E_n(0) - E_G(0)}$$

where suffixes i, j stand for x, y or z.

Hence

$$H'_{M_s, M_s'} = [\langle M_s | (\beta\vec{H} + \lambda\vec{S}) \cdot \underset{\sim}{\Lambda} \cdot (\beta\vec{H} + \lambda\vec{S}) | M_s' \rangle] \\ = \langle M_s | \beta^2 \vec{H} \cdot \underset{\sim}{\Lambda} \cdot \vec{H} + \lambda^2 \vec{S} \cdot \underset{\sim}{\Lambda} \cdot \vec{S} + 2\beta \vec{H} \cdot \Lambda \cdot \vec{S} | M_s' \rangle \qquad (2.23)$$

The first term on R.H.S. of equation of (2.23) gives temperature independent paramagnetism and is neglected[3]. Taking into account the energy term from the first order, the resulting Hamiltonian can be written[3] as

$$H_s = \beta\vec{H}\cdot g_e\cdot\vec{S} + \lambda^2\vec{S}\cdot\underset{\sim}{\Lambda}\cdot\vec{S} + 2\beta\lambda\vec{H}\cdot\underset{\sim}{\Lambda}\cdot\vec{S}$$

$$= \beta\vec{H}\,(g_e\cdot I + 2\lambda\underset{\sim}{\Lambda}\,)\cdot\vec{S} + \lambda^2\vec{S}\cdot\underset{\sim}{\Lambda}\cdot\vec{S}$$

$$= \beta\vec{H}\cdot\underset{\sim}{g}\cdot\vec{S} + \vec{S}\cdot\underset{\sim}{D}\cdot\vec{S} \qquad (2.24)$$

Here I is the unit tensor, $\underset{\sim}{g} = g_e\underset{\sim}{I} + 2\lambda\underset{\sim}{\Lambda}$ and $D = \lambda^2\cdot\underset{\sim}{\Lambda}\cdot\vec{S}$ is an operator which corresponds to the effective spin. The value of the effective spin S is determined by equating the total number of components of the ground state which are responsible for paramagnetic resonance absorption to $2S+1$. The effective spin is used in the calculation of the constants in the spin-Hamiltonian developed by Pryce[4] and Abragam and Pryce[5] for transition metal ions of the group. For an orbitally singlet state the splitting of spin degeneracy is small and effective spin is taken as equal to the actual spin. It is obvious that if $\lambda = 0$, the tensor $\underset{\sim}{g}$ should be isotropic with the value 2.00232. Any deviation from this value involves contribution from the tensor $\underset{\sim}{\Lambda}$ which is nothing but the contribution from the excited state.

The spin-spin interaction is also represented[3] by $\vec{S}\cdot\underset{\sim}{D}\cdot\vec{S}$ which is effective for $S \geq 1$ and thus it is not possible to separate it from the analogous term in equation (2.24). The expression $\vec{S}.\underset{\sim}{D}.\vec{S}$ can be put in an alternative form as shown[3] below

$$\vec{S}\cdot\underset{\sim}{D}\cdot\vec{S} = D_{xx}S_x^2 + D_{yy}S_y^2 + D_{zz}S_z^2$$

in the principal axis system. It can be arranged as

$$= D[S_z^2 - (1/3)\,S(S+1)] + E(S_x^2 - S_y^2) +$$

$$+(1/3)[(D_{xx} + D_{yy} + D_{zz})\,S(S+1)]$$

Here $D = D_{zz} - (D_{xx} + D_{yy})/2$, and $E = (D_{xx} - D_{yy})/2$

$\underset{\sim}{D}$ is a traceless tensor making $D_{xx} + D_{yy} + D_{zz} = 0$. It is seen that for axial symmetry, $E = 0$, and for cubic symmetry $D = 0$ also. However, in the case of cubic symmetry there will be fourth order terms, which are normally very small in the cases of strong axial symmetry, to make the Hamiltonian invariant under cubic point group. Therefore, taking the h.f. interactions into account, the total Hamiltonian can be written as[3]

$$\mathcal{H} = \beta(g_x H_x S_x + g_y H_y S_y + g_z H_z S_z) + D[S_z^2 - (1/3)S(S+1)$$
$$+ E(S_x^2 - S_y^2) + (a/6)[S_x^4 + S_y^4 + S_z^4 - (1/5)S(S+1)$$
$$\cdot (3S^2 + 3S - 1)] + (F/180)[35S_z^4 - 30S(S+1)S_z^2$$
$$+ 25S_z^2 - 6S(S+1) + 3S^2(S+1)^2] + A_z I_z S_z + A_x I_x S_x$$
$$+ A_y I_y S_y + Q'[I_z^2 - (1/3)\, I(I+1)] + Q''(I_x^2 - I_y^2)$$

Here a and F are fine structure constants, $Q' = 3Q_{zz}/2$, $Q'' = (Q_{xx} - Q_{yy})/2$ and A_x, A_y and A_z are principal values of hyperfine tensor.

ZERO-FIELD SPLITTING OF S STATE IONS

The ground state of Mn^{2+} ion is $3d^5\ {}^6S_{5/2}$. Since the electronic charge distribution of the S-state is spherically symmetric, the crystal field will not split this state. Further, since the total orbital angular momentum $L = 0$, the spin-orbit coupling will not, to a first order, split its six fold spin degeneracy. The zero field splitting of this state, however, is known since long. The group theoretical treatment of Bethe[2] indicates that this state with $J = 5/2$ gets split even in a cubic field, into two components- a doubly degenerate and a quartely degenerate. A further distortion of this field can cause

the splitting of quartet into two doublets. Thus in a field of axial symmetry or lower symmetry, zero field splitting gives three Kramer's doublets. The degeneracy of these levels is lifted in the presence of magnetic field as shown in Fig. 2.3.

The mechanism of zero field splitting of S state ion in crystalline environment has been studied by several workers. The origin of splitting of this state was first discussed by the Van Vleck and Penny[7]. They considered higher order admixtures involvin spin orbit coupling. The mechanisms proposed by Pryce[8] involves spin-spin interaction and admixture of state from $3d^4$ 4s configuration. Watanabe[9] considered spin-spin and spin-orbit interaction between states of $3d^5$ configuration responsible for zero field splitting. Blume and Orbach[10] mechanism involves spin-orbit admixture of excited $|^4P\rangle$ into ground $^6S_{5/2}$ state in the axial field splitting of deformed cubic host.

Wybourne[11] used relativistic wave functions in the calculation of crystal field matrix element using L-S basis states for the angular part and Hartree-Fock type wave functions for the radial part. Sharma et al,[12] took into account the spin-spin, and spin-orbit interaction together with overlap effect for calculating the magnetude

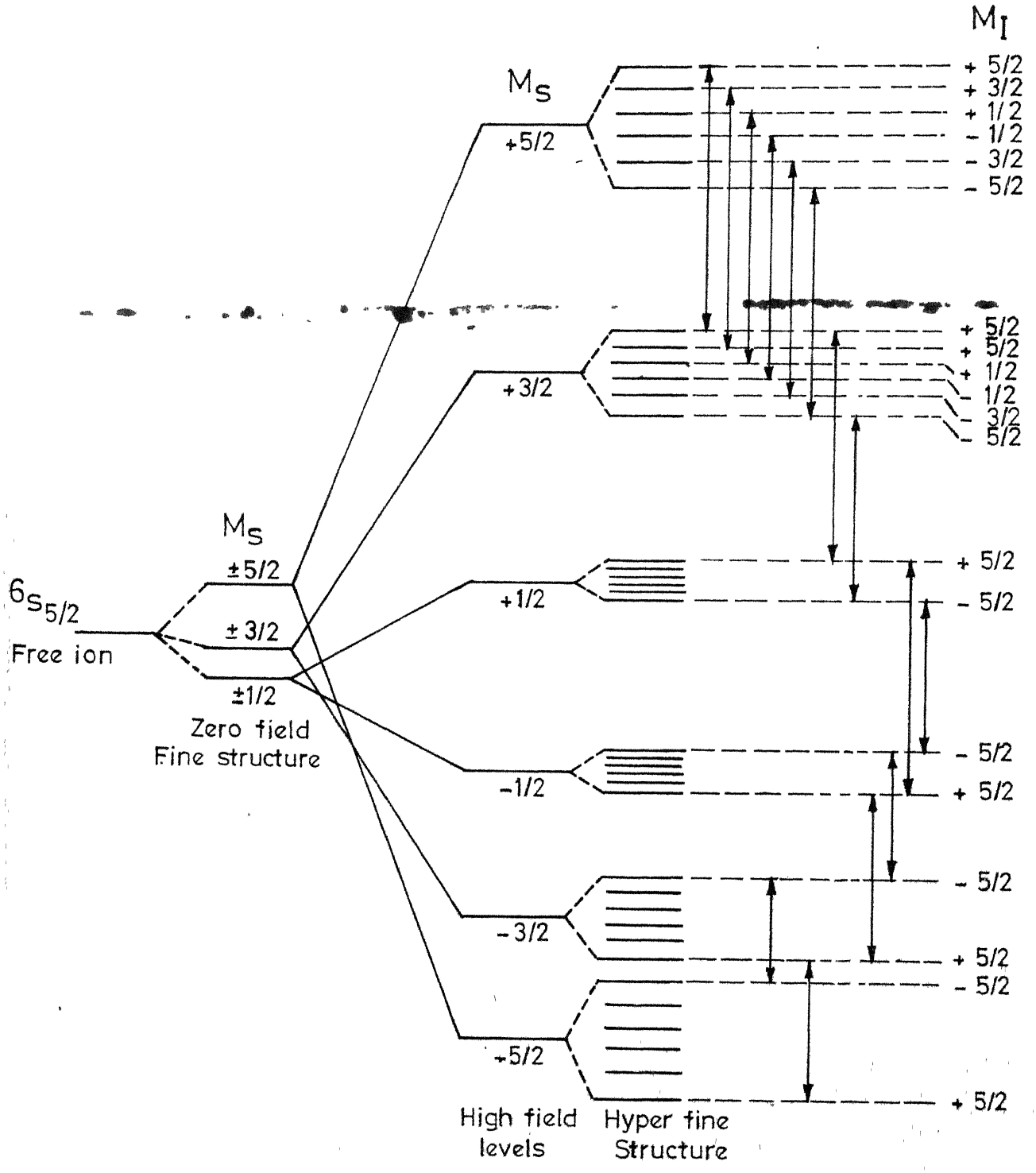

Fig. 2.3 A schematic energy-level diagram of Mn^{2+} ion showing electronic levels in zero and strong magnetic field together with splitting due to nuclear spin. Some of the typical transitions, $\Delta M_S = \pm 1$ $\Delta M_I = 0$ are indicated by arrows.

and sign of the zero field splitting parameters D and E. Srivastava[13] proposed phonon induced crystal field effect for cubic field splitting of this state. In general, the zero-field splitting is due to all effects mentioned above though the relative contributions are different.[14]

A pure S-state will show no hyperfine splitting firstly because its orbital angular momentum and therefore its orbital magnetic moment is zero and secondly because the magnetic field produced at the site of nucleus due to the spin of spherically distributed electronic charge around the nucleus, is zero. Abragam[15] proposed that the observed h.f. splitting may be due to configuration interaction of $3s\ 3d^5\ 4s$. The s-electron has nonvanishing spin density at the nucleus and therfore may contribute to Fermi or contact interaction. Orbitals such as p and d have nodal planes passing through nucleus and therefore have zero spin density. The contribution to the magnetic field due to electron at the site of nucleus may come through core polarization. The two s-electrons of 3s orbital are coupled electrostatically to 3d electrons. The wave functions of these two electrons differ from each other by an exchange term and consequently they are not paired off completely. This may give rise to magnetic field at the nucleus. The interaction between nuclear and electronic magnetic field may give rise to hyperfine splitting.

REFERENCES

1. Peter B. Ayscough 'Electron Spin Resonance in Chemistry' Butler and Tanner Ltd., Frome and London (1967) p. 31

2. H.A. Bethe, Annls, Phys. 3, 133 (1929) (English Translation, Consultants Bureau, New York (1958).

3. J. E. Wertz and J. R. Bolton, 'Electron Spin Resonance Theory and Practical Application', Els. McGraw-Hill, Inc., 1972) p. 266; A. Abragam and B. Bleaney, Electron Paramagnetic Resonance of Transition Ions, Clarendon Press, Oxford (1970).

4. M. H. L. Pryce, Proc. Phys. Soc. (London) 463,25 (1950).

5. A. Abraham and M. H. L. Pryce, Proc. Roy. Soc. (London) A205, 135 (1952).

6. W. Low 'Paramagnetic Resonance in Solids' (Academic Press New York and London 1960) P. 46.

7. J. H. Van Vleck and W. G. Penney, Phil. Mag. 17, 961 (1934).

8. M. H. L. Pryce, Phys. Rev. 80, 1107 (1950).

9. H. Watanabe, Progr. Theoret Phys. (Kyoto) 18, 405 (1937).

10. M. Blume and R. Orbach, Phys. Rev. 127, 1987 (1962)

11. B. G. Wybourne, J. Chem. Phys. 43, 4506 (1965).

12. R. R. Sharma, T. P. Dass and R. Orbach, Phys. Rev. 149, 257 (1966), 155, 338 (1967).

13. A. M. Srivastava, Phys. Rev. 187, 446 (1969).

14. R. Janakiraman, Electron Paramagnetic Resonance of Mn^{2+} in some Dia and Paramagnetic single Crystals, Ph.D. Thesis, Indian Institute of Technology Kanpur (1970).

15. A. Abragam, Phys. Rev. 79, 534 (1950).

CHAPTER 3

ELECTRON PARAMAGNETIC RESONANCE OF Mn^{2+} ION IN DIAMMONIUM OXALATE MONOHYDRATE SINGLE CRYSTAL

ABSTRACT

The electron paramagnetic resonance of Mn^{2+} ion in single crystals of diammonium oxalate monohydrate has been investigated for the first time. This study indicates that Mn^{2+} ion substitutes for NH_4^+ ion in the crystal lattice and is associated with first neighbour NH_4^+ vacancy such that the Z-axis of the complex lies in a b plane. The spectrum has been fitted to a spin-Hamiltonian appropriate for orthorhombic symmetry.

INTRODUCTION

The electron paramagnetic resonance of Mn^{2+} ion doped in a single crystal of diammonium oxalate monohydrate $[(NH_4)_2C_2O_4.H_2O]$ has been studied at room temperature. No EPR study seems to have been made on this crystal doped with impurity ions. However, EPR study of γ-irradiated crystal has been reported[1] and it shows the formation of $C_2C_4^-$ radical derived from $C_2O_4^{--}$ ion and OH radical derived from the water molecule in the crystal lattice.

EXPERIMENTAL PROCEDURE

Single crystals of diammonium oxalate monohydrate doped with Mn^{2+} ion were grown from the aqueous solution of salt containing about 1 percent of $MnCl_2$ by weight evaporating the solution in a dessicator containing concentrated sulphuric acid at room temperature. The crystals were transparent and prismatic in shape with the growth axis along the c-axis of the crystal. This axis was confirmed by x-ray rotation picture taken with a Weisenberg camera. The crystal used for the EPR study had dimensions 0.5 x 0.1 x 0.1 cm^3.

The EPR spectra were recorded with a Varian V-4502 EPR spectrometer. The magnetic field was produced

by a Varian 12 inch electromagnet and modulated at 100 kHz. The cylindrical as well as rectangular resonant cavities were used. The spectra were recorded with a dual channel strip chart recorder. The frequency of the klystron was measured with Hewlett Packard frequency meter, Model X532 B. DPPH was used as a field marker.

CRYSTAL STRUCTURE

The crystal structure of diammonium oxalate monohydrate has been studied in detail by X-ray[2] and neutron diffraction[3] techniques. The crystal belongs to an orthrhombic system and its space group is $D_2^3(P2_12_12)$. In the ab plane of the crystal lattice, there are four screw diads, a set of two being parallel to the crystal a-axis and the other two to b-axis. There are four ammonium ions in the unit cell.

The X-ray analysis places all atoms except the oxygens of water molecules in the general positions of the $D_2^3(P2_12_12)$ space group:

$$xyz\ ;\ \bar{x}\,\bar{y}\,z\ ;\ x+1/2, 1/2-y, \bar{z}\ ;\ 1/2-x, y+1/2, \bar{z}$$

with the following parameters.[4]

C	:	x = 0.092,	y = 0.027,	z = 0.066
O(1)	:	x = 0.200,	y = -0.056,	z = 0.140
O(2)	:	x = 0.118,	y = 0.142,	z = 0.001
NH_4	:	x = 0.386,	y = 0.228,	z = 0.424

The water molecules are situated at 0, 1/2, u; 0, $\bar{u}$ with u = 0.192. The above parameters are referred to the unit cell dimensions

$$a = 8.04 \text{ Å}, \quad b = 10.27 \text{ Å}, \quad c = 3.82 \text{ Å}$$

The structure of diammonium oxalate monohydrate projected on the basal plane is shown in Fig. 3.1.

RESULTS AND DISCUSSION

The electronic configuration of Mn^{2+} is $3d^5$ and consequently the ground state of the free ion is $^6S_{5/2}$. This state is orbitally nondegenerate but has six-fold spin degeneracy. Under the action of the crystalline field of orthorhombic symmetry or lower symmetry, this degenerate state is splits into three Kramers' doublets which are further split into six levels under a static magnetic field. The EPR spectrum of Mn^{2+} ion in such an environment is expected to show five fine structure transitions and each of these will consist of six hyperfine components due to nuclear spin I = 5/2. Figures 3.2, 3.3 and 3.4 show the

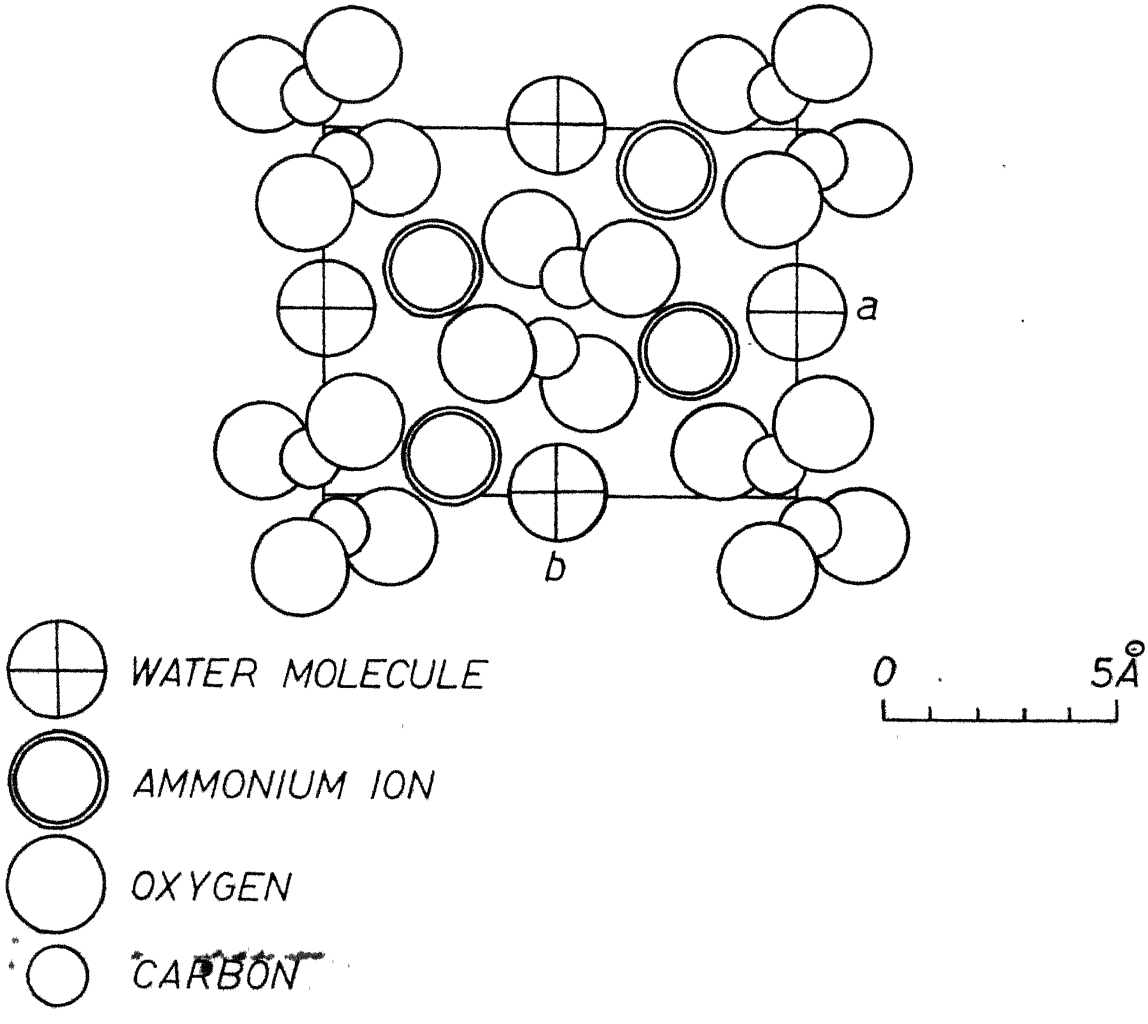

FIG. 3.1 THE STRUCTURE OF $(NH_4)_2C_2O_4.H_2O$ PROJECTED ON THE BASAL PLANE[4] ab.

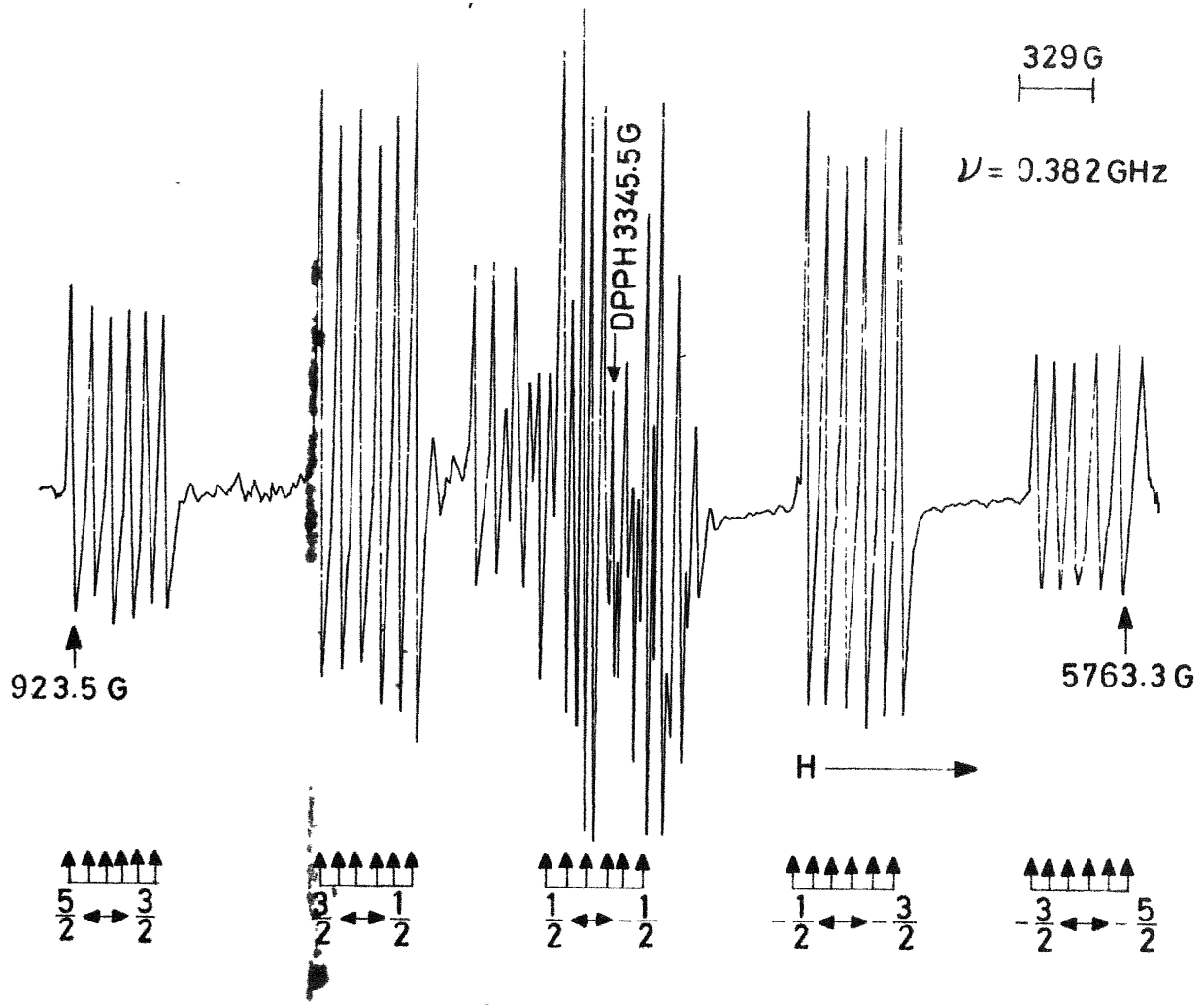

FIG. 3.2 THE EPR SPECTRUM OF Mn^{2+} IONS DOPED IN $(NH_4)_2Cu_2O_4 \cdot H_2O$ SINGLE CRYSTAL WITH H ALONG Z-AXIS OF ONE OF THE SITES AT ROOM TEMPERATURE. THE COALASCED SPECTRUM (CORRESPONDING TO $\theta = 60^\circ$) OF THE SECOND SITE IS SEEN IN THE MIDDLE OF THE SPECTRUM.

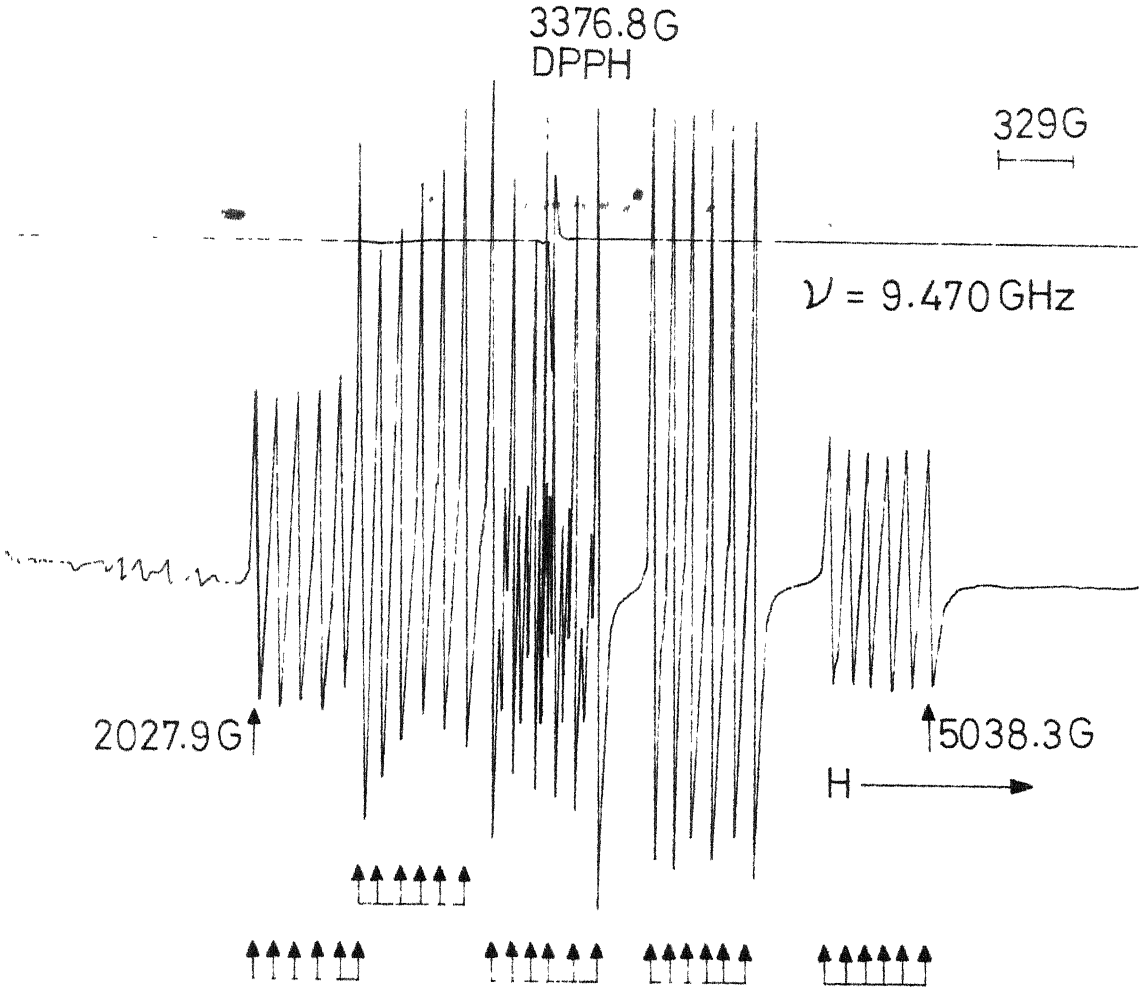

FIG. 4.X ... EPR SPECTRUM OF Mn^{2+} ION DOPED IN $(NH_4)_2C_2O_4 \cdot H_2O$ ... CRYSTAL ... MAGNETIC FIELD ALONG X-AXIS AT ... TEMPERATURE. THE EXTRA LINES SEEN IN THE CENTRAL PART OF THE SPECTRUM ARE DUE TO THE SECOND SITE.

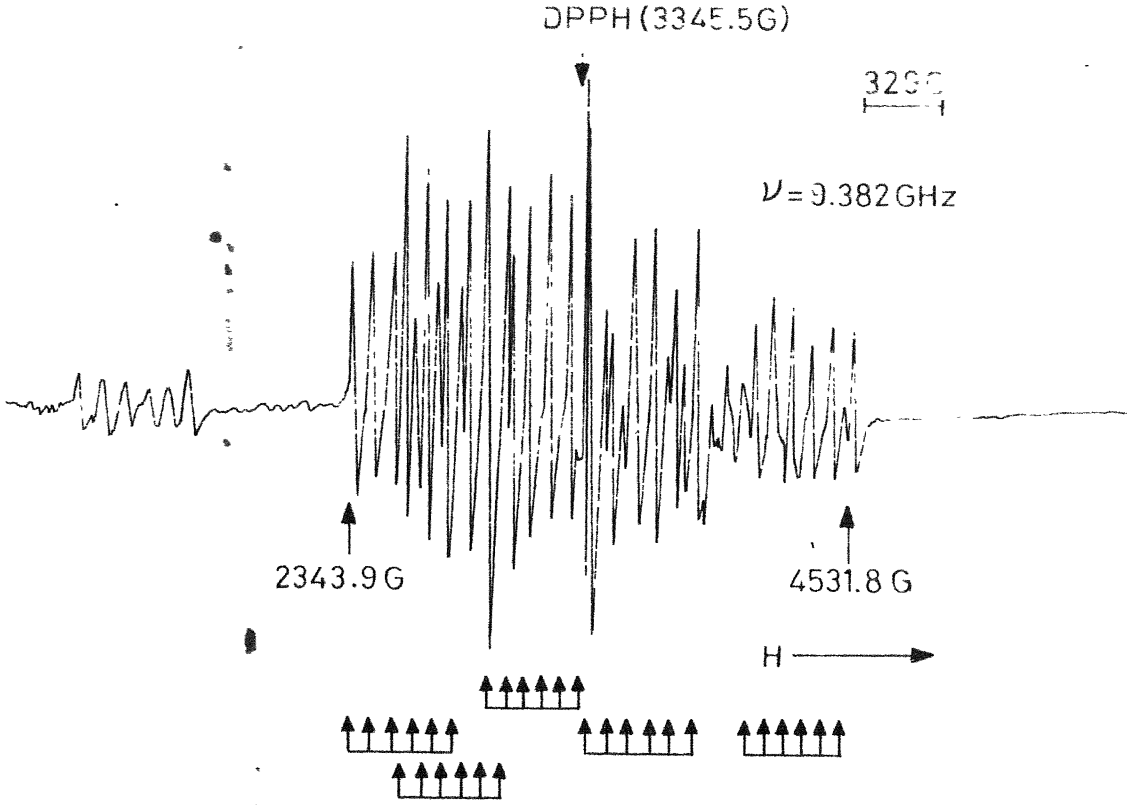

FIG. 3.4 THE EPR SPECTRUM OF Mn^{2+} ION DOPED IN $(NH_4)_2C_2O_4 \cdot H_2O$ SINGLE CRYSTALS WITH MAGNETIC FIELD ALONG Y-AXIS OF ONE OF THE SITES AT ROOM TEMPERATURE. THE 'HYPERFINE SET' SEEN AT THE LOW FIELD SIDE SHOWS UNEVEN HYPERFINE SPACING WHICH DECREASED WITH INCREASE OF H. THIS IS IN CONTRAST TO THE OTHER HYPERFINE SET SHOWN IN THIS FIGURE. THE LOW FIELD TRANSITION IS PROBABLY DUE TO AN ELECTRONICALLY FORBIDDEN TRANSITION.

Z, X, and Y-axes spectra respectively of Mn^{2+} ion in $(NH_4)_2C_2O_4.H_2O$ single crystals at room temperature. The Z-axis spectrum, corresponding to the maximum spread has been obtained by rotating the crystal in different planes using two-plane goniometer. Z-axis has been found to lie in the crystallographic ab plane. X and Y axes are located by studying the angular variation in the ab plane and in a plane obtained by making the c-axis horizontal with the help of two plane goniometer[5] and looking for the extreme separated by 90°. The angular variation further revealed the existence of two identical Z-axis spectra at an angular separation of 60° in ab plane. On further rotation of the crystal in this plane no such spectrum was obtained till 180° part of the first Z-axis spectrum appeared. The angular variation of the spectrum for one complex in ZX plane is shown in Fig. 3.5. This clearly indicates the existence of two physically identical complexes which are magnetically inequivalent for a random direction, with their Z-axes separated by an angle of 60° in the ab plane. The most probable site which Mn^{2+} ion will occupy is a substitutional position at NH_4^+ site. In figure 3.6, the positions of four ammonium ions in the unit cell are marked by I, II, III and IV. The ammonium ions marked

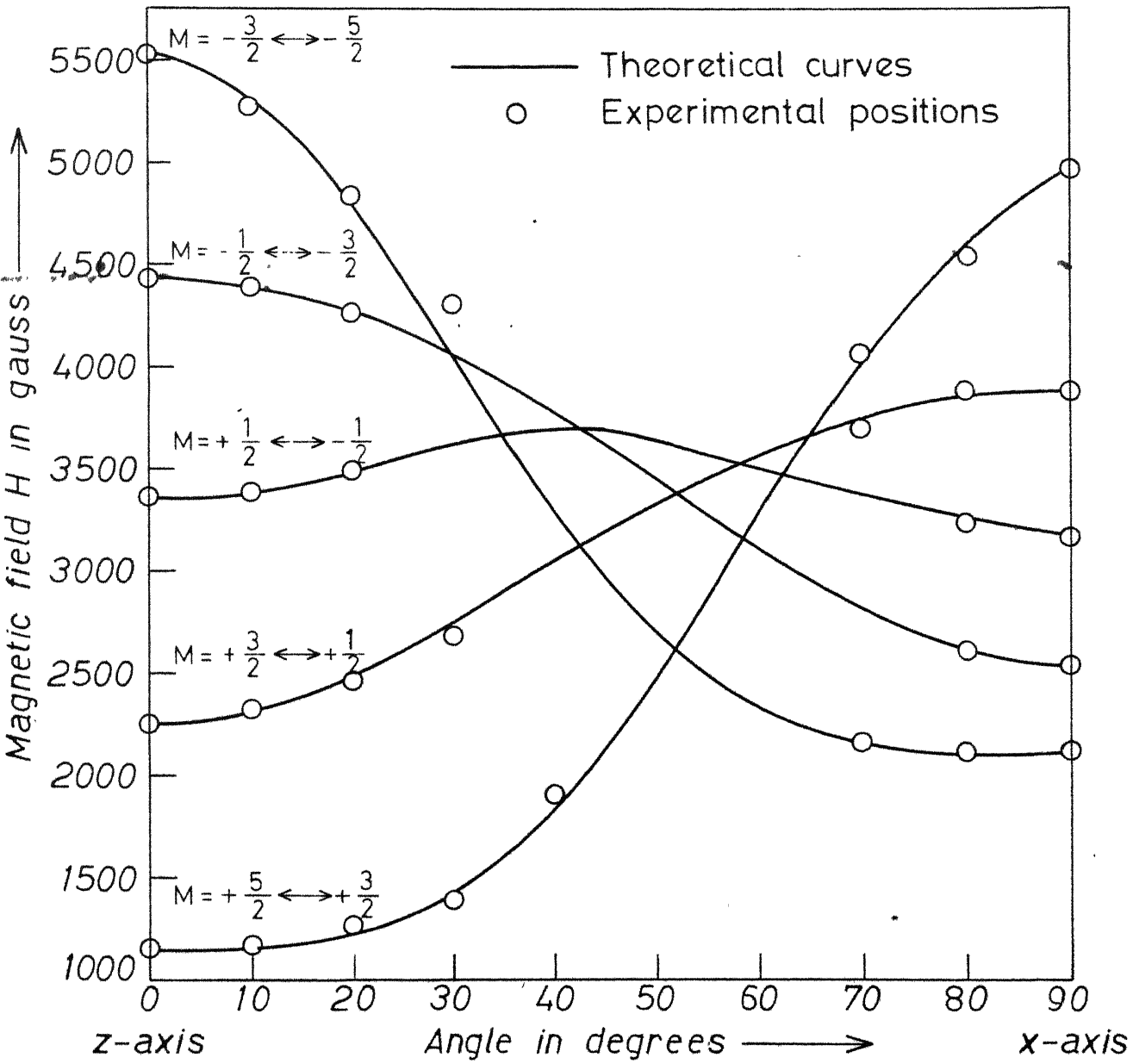

FIG. 3.5 ANGULAR VARIATION OF THE ALLOWED FINE STRUCTURE TRANSITIONS IN THE ZX PLANE OF THE ONE OF THE MAGNETIC COMPLEXES OF Mn^{2+} IN $(NH_4)_2C_2O_4.H_2O$ SINGLE CRYSTALS.

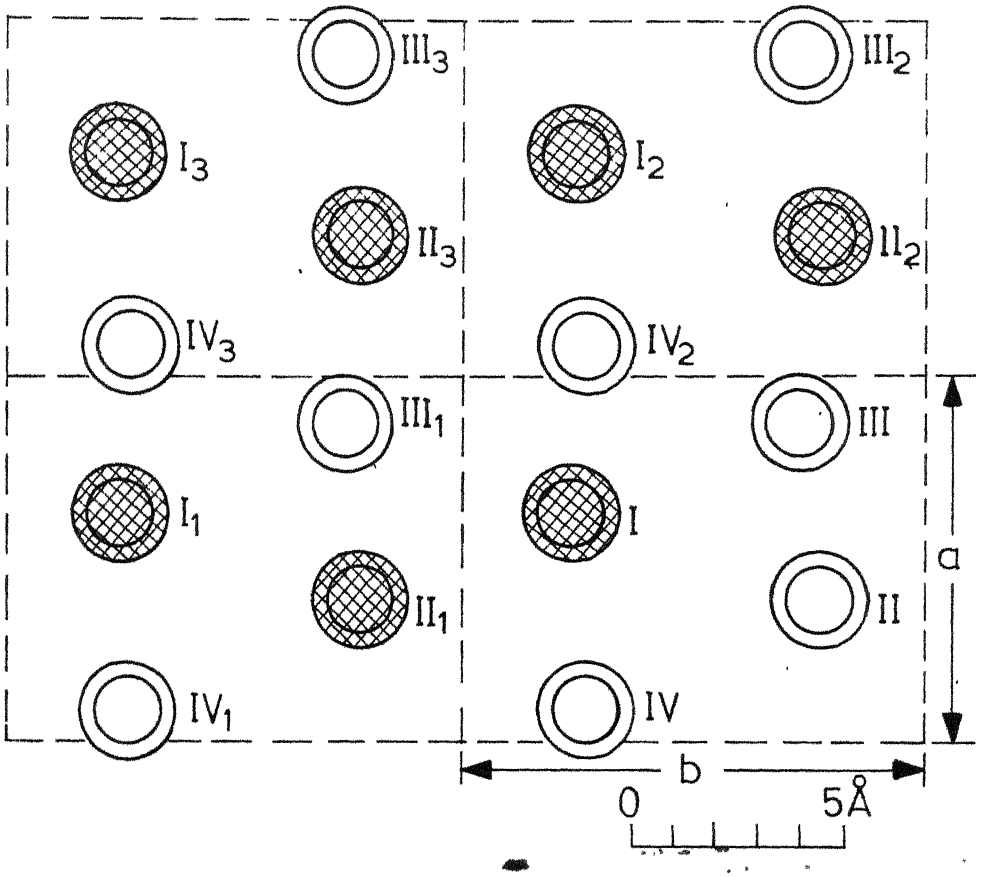

FIG. 3.6 PROJECTION OF AMMONIUM IONS IN THE ab PLANE SHOWING FOUR ADJOINING UNIT CELLS OF DIAMMONIUM OXALATE MONOHYDRATE. SHADED RINGS REPRESENT NH_4^+ IONS ABOVE THE PLANE OF THE PAPER AND UNSHADED ONES REPRESENT IONS BELOW THE PLANE OF THE PAPER.

by I and II in Fig. 3.6 are related by C_2 symmetry about the c-axis, and so also those marked by III and IV. These two sets are not quite independent and are related by screw diads. If Mn^{2+} occupies a NH_4^+ site and is not associated with any charge compensating defects the spectrum essentially should reflect the symmetry of the crystal with c-axis (C_2) as the Z-axis. However, this has not been the case. The observation of a complex having two possible orientations such that the corresponding Z-axes are separated by about 60^o in the ab plane is consistent with the following model. Mn^{2+} occupies the NH_4^+ ion sites I (or II) and is associated with a first neighbour cation vacancy at II_1. A symmetry related configuration of such a Mn^{2+} - vacancy complex will be Mn^{2+} at III associated with a vacancy at IV_2. This is illustrated in Fig. 3.7 This results in two magnetically inequivalent complexes having Z-axes separated by 60^o in the ab plane. A similar model with second neighbour cation vacancies either in ab plane or out of ab plane does not result in the observed behaviour and hence it has not been considered.

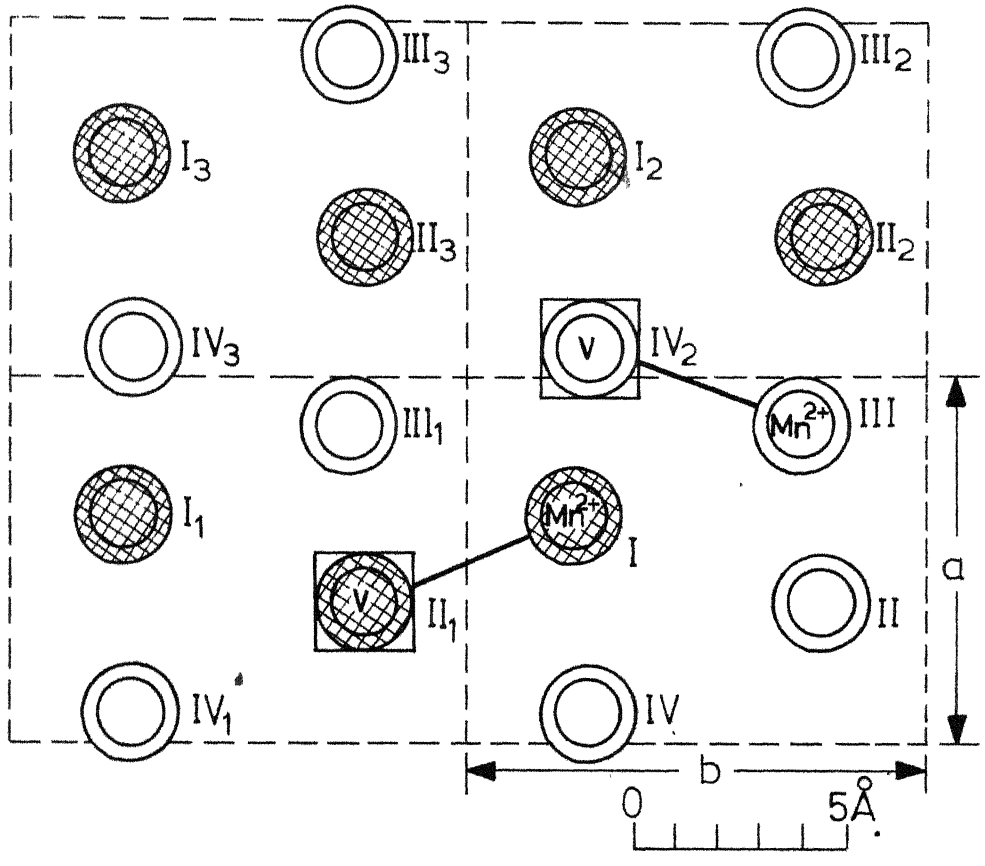

FIG. 3.7 PROJECTION OF AMMONIUM IONS IN THE ab PLANE SHOWING FOUR ADJOINING UNIT CELLS OF DIAMMONIUM OXALATE MONOHYDRATE SHADED RINGS REPRESENT NH_4^+ IONS ABOVE THE PLANE OF THE PAPER AND UNSHADED ONES REPRESENT THOSE BELOW THE PLANE OF THE PAPER. A TWO POSSIBLE Mn^{2+} - VACANCY PAIRS IN TWO ADJOINING UNIT CELLS ARE SHOWN. Mn^{2+} IS IN THE SUBSTITUTIONAL POSITION. [V] STANDS FOR VACANCY OF NH_4^+ ION.

The Z-, Y- and X-axes spectra of Mn^{2+} ion ($S = 5/2$, $I = 5/2$) corresponding to transitions $\Delta M_s = \pm 1$, $\Delta m_I = 0$ were analysed using the spin-Hamiltonian[6]

$$\mathcal{H} = \beta g_z H_z S_z + \beta g_x h_x S_x + \beta g_y H_y S_y + D[S_z^2 - (1/3)S(S+1)] + E(S_x^2 - S_y^2) + A_z S_z I_z + A_x S_x I_x + A_y S_y I_y$$

The suffixes x, y and z represent corresponding components along principal axes. In case of D and E << Zeeman term and E << D, the terms upto third order as given by Chambers et al[5] were found sufficient for this system. The resonance magnetic fields for different transitions for the magnetic field along Z-direction of the crystalline field are given[6] below:

(a) Fine Structure transitions.

$$H(M_s = \pm 5/2 \leftrightarrow \pm 3/2) = H_o \mp 4D + 4\frac{E^2}{H_o} \pm 6\frac{DE^2}{H_o^2} + \frac{36D^2E^2}{H_o^3} + \frac{28E^4}{H_o^3}$$

$$H(M_s = \pm 3/2 \leftrightarrow \pm 1/2) = H_o \mp 2D - \frac{5E^2}{H_o} \pm \frac{33DE^2}{H_o^2} + \frac{45D^2E^2}{H_o^3} - \frac{5}{4}\frac{E^4}{H_o^3} \quad (3.1)$$

and $$H(M_s = +1/2 \leftrightarrow -1/2) = H_o - \frac{8E^2}{H_o} + \frac{72D^2E^2}{H_o^3} + \frac{56E^4}{H_o^3}$$

(b) Hyperfine Transitions

$$H(M_s,\ m_I \leftrightarrow M_s \pm 1,\ m_I) = -Am_I - \frac{B^2}{2H_o} \cdot \left[\frac{35}{4} - m_I^2 + m_1(2M_s - 1)\right] \qquad (3.2)$$

where $A = A_z$ and $B = \frac{(A_x + A_y)}{2}$

When the magnetic field is along the X-or the Y-axis, the above equations are modified[7] by replacing D by 1/2 (3E - D), and E by (1/2) (D + E) for H along X-axis; and D by -1/2 (D + 3E) and E by 1/2 (D-E) for H along Y-axis.

In evaluating the spin-Hamiltonian parameters from the Z-axis spectra four fine structure positions have been used. The position of the central (+ 1/2 ↔ - 1/2) transition could not be accurately determined due to overlap of other lines from the second site. The values of H_o were approximately calculated from the expressions for extreme fine structure positions H_1 and H_5, and also the next H_2 and H_4, neglecting higher order terms in these expressions. A rough estimate of D was made by averaging its value obtained from the differences of H_1 and H_5 and H_2 and H_4, neglecting higher order terms in these expressions.

The value of D obtained from the Z-axis spectrum was further more accurately calculated taking into account the contribution from higher order terms using average value of E of X- and Y-axis spectra. The value of E could not be estimated from the Z-axis spectrum since there is no linear term in E and contribution from the $\frac{E^2}{H_0}$ term is very small. The values of (D+3E) from the Y-axis spectrum was first estimated roughly by taking the difference of H_4 and H_2, H_5 and H_1 and (D-E) from the H_3. The equation (3.1) were used to estimate D and E. Further refinement was made by taking into account the contribution from higher order terms in the transformed expression for Y-axis spectrum. A similar procedure was adopted to get the refined values of D and E. From the X-axis spectrum the values of H_o were obtained by adding H_5 and H_1, H_4 and H_2, taking into account the contributions from higher order terms involving D and E. The spin-Hamiltonian parameters calculated from the X, Y and Z axis spectra are given in Table 3.1. The consistency of the parameters obtained is satisfactory.

Table 3.1. The spin Hamiltonian parameters for Mn^{2+} doped in $(NH_4)_2C_2O_4.H_2O$

	Z	Y	X
D(cm^{-1})	513×10^{-4}	511×10^{-4}	511×10^{-4}
E(cm^{-1})	+	37×10^{-4}	32×10^{-4}
g	2.0069	2.0099	2.007
A(cm^{-1})	82×10^{-4}	84×10^{-4}	87×10^{-4}

+ The value of E from Z-axis spectrum could not be calculated due to small value of $-\frac{E^2}{H_o}$ term. E does not appear in linear form in the expressions for Z-axis fine structure transitions, $\Delta M_s = \pm 1$.

REFERENCES

1. M. V. Krishnamurty, Mol. Phys. 24, 1353 (1972).

2. J. H. Robertson, Acta Crystallogr. 18, 410 (1965).

3. V. M. Padmanabham, S. Sribanta and S. Medhi Ali, Acta Crystallogr. 18, 576 (1965).

4. Ralph W. G. Wyckoff, Crystal Structure, Vol. 5 (Inter Science Publishers, 2nd Edition p. 412).

5. R. Janakiraman, 'Electron Paramagnetic Resonance studies of Mn^{2+} in some Dia and Paramagnetic single Crystals' Ph.D. Thesis, Indian Institute of Technology Kanpur India (1970).

6. J. G. Chambers, W. R. Datars and C. Calvo, J. Chem. Phys. 41, 306 (1964).

7. A. V. Jagannadham, 'Electron Paramagnetic Resonance of Mn^{2+} and Vo^{2+} ion in single crystals'- Ph.D. Thesis Indian Institute of Technology, Kanpur, India(1969).

CHAPTER 4

ELECTRON PARAMAGNETIC RESONANCE STUDY OF VO^{2+} IN KH_2PO_4 SINGLE CRYSTAL

ABSTRACT

The electron paramagnetic resonance of VO^{2+} ion in KH_2PO_4 single crystal at room temperature has been studied. The EPR results suggeste the formation of two vanadyl complexes in KH_2PO_4 lattice. One of the these complexes seems to be the well known $[VO(H_2O)_5]^{2+}$ which probably has been trapped in an orderly way in the crystal lattice. For the other centre, VO^{2+} ion seems to have entered the lattice interstitially resulting in the formation of a square bipyramidal type of vanadium.

INTRODUCTION

The electron paramagnetic resonance of VO^{2+} ion has been observed in distorted octahedral environments of hexahydrate complexes, the examples being alkali alums[1,2] and Tutton salts.[3] In alums trivalent cations are surrounded by nearly regular octahedra of water molecules where as in Tutton salts, the divalent cations have such octahedral surroundings. On doping the alums[1,2] with vanadyl salts, VO^{2+} substitutes for trivalent cations in alums and forms a complex $[VO(H_2O)_5]^{2+}$ replacing one water molecule by oxygen of V-O. VO^{2+} ion entering in TiO_2[4] and GeO_2[5] lattices is surrounded by a distorted octahedron of oxygens. Banerjee[5a] carried out preliminary work in this laboratory a few years ago on the EPR of VO^{2+} in Potassium dihydrogen phosphate (KDP) single crystals, but no definite progress could be made in understanding the system at that time. A detailed study has now revealed the existence of two types of vanadium complexes in KDP crystals and the present chapter deals with the results obtained in this connection.

CRYSTAL STRUCTURE

Potassium dihydrogen phosphate belongs to a tetragonal system at room temperature and its space group is $D_{2d}^{12} - I\bar{4}\,2d$. There are four molecules of KH_2PO_4 in its unit cell. In the ferroelectric phase (Curie temp.

$T_c = 123^oK$) the crystal belongs to an orthorhombic system of class C_{2v}^{19}- Fdd. The crystal structure was first studied by West[7] using X-ray techniques. The dimensions of the unit in the tetragonal phase determined more accurately by Ubbelhode and Woodward[8] are as follows:

$$a = b = 7.434 \text{ Å}, \quad c = 6.954 \text{ Å}$$

The atomic coordinates in the unit cell are given in the table 4.1.

Table 4.1. Positions of atoms in the unit cell of KH_2PO_4

Lattice points	Coordinates
4(P)	0,0,0; 1/2,0,1/4; 1/2,1/2,1/2; 0,1/2,3/4
4(K)	0,0,1/2; 1/2,0,3/4; 1/2,1/2,0; 0,1/2, 1/4
16(O)	x,y,z; 1/2 - x,y, 1/4-z, $\bar{x},\bar{y},z$; 1/2 + x,y, 1/4-z $\bar{y},\bar{x},z$; 1/2 + y,x, 1/4+z y,x,$\bar{z}$; 1/2 - y,$\bar{x}$, 1/4+z; plus eight similar points about 1/2,1/2,1/2.

The parameters of oxygen determined accurately by neutron diffraction technique are x = 0.0828 y = 0.1436, z = 0.1261.

The PO_4 groups are nearly regular tetrahedra. Every phosphate group is linked to four neighbouring groups by hydrogen bonds. The length of O- H- O bond is about 2.5 Å. The hydrogen bond in the lattice is such that it links an oxygen belonging to an upper phosphate group to a neighbouring oxygen belonging to a lower phosphate group. Each hydrogen bond lies very nearly perpendicular to the c-axis. In the paraelectric phase, the information about the location of hydrogen is given by neutron diffraction analysis which shows a peak of scattering density midway between thetwo oxygens linked by hydrogen bond. The peak is found elongated along the axis of the bond. This fact may be explained either by taking the thermal amplitude of vibration of the hydrogen atom to be larger along the bond direction or by taking statistical distribution of hydrogen over two positions of equilibrium on the bond, which are about 0.40 Å apart. The infra-red and Raman investigations indicate the validity of the second interpretation. The structure of the unit cell of KH_2PO_4 in the space group $I\bar{4}2d^7$ is given in Fig. 4.1.

In order to compare the Fdd system below the Curie point with the tetragonal phase I $\bar{4}$2d system,

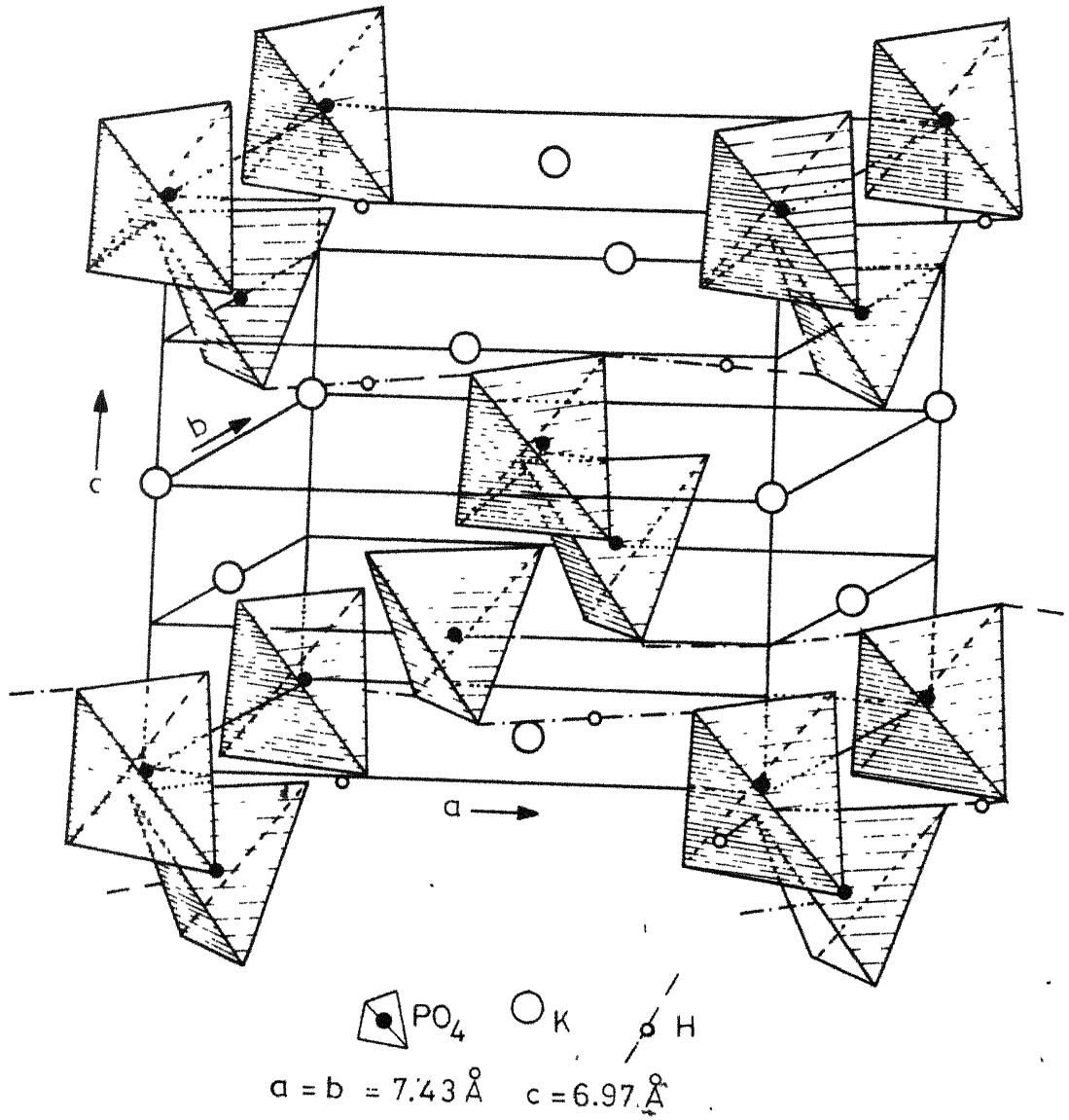

FIG. 4.1 STRUCTURE OF KH_2PO_4 UNIT CELL IN SPACE GROUP $I\bar{4}2d$.

it is convenient to introduce the alternative F $\bar{4}$d2 representation of the tetragonal cell. This unit cell contains 8 molecules of KH_2PO_4. The dimensions for the unit cell in the F $\bar{4}$d2 (tetragonal) system are then a=b=10.48 Å, c = 6.90 Å, while in the Fdd (orthorhombic) system they are a = 10.53 Å, b = 10.44 Å, c = 6.90 Å.

THEORY

A tetravalent vanadium ion with outer electronic configuration $3d^1$ exists in a most stable form as VO^{2+}, the bonding of vanadium with oxygen being highly covalent. Ballhausen and Gray[7] considering the LCAO-MO description of this molecular ion in the complex $VO(H_2O)_5^{2+}$ have shown that an unpaired d-electron occupies a non-bonding b_2 type orbital ($3d_{xy}$) and thus the lowest state becomes a singlet state. Thus, for the $3d_{xy}$ state one can expect only one electronic transition. Because of magnetic interaction of the electron with the vanadium nucleus (51_V) with I = 7/2, the EPR spectrum shows eight characteristic hyperfine lines.

The EPR spectrum of VO^{2+} ions in an axial field can be described by the spin-Hamiltonian[2]

$$\mathcal{H} = g_{\parallel} \beta H_z S_z + g_{\perp} \beta (H_x S_x + H_y S_y) + A I_z S_z + B(I_x S_x + I_y S_y) \qquad (4.1)$$

with S = 1/2 and I = 7/2.

The above Hamiltonian gives the resonance magnetic field positions of the hyperfine lines[8] to second order in A and B as

$$H = H_o - \frac{Km_I}{g\beta} - \frac{B^2(A^2+K^2)}{4H_o g^2 B^2 K^2}\,[I(I+1)-m_I^2] \qquad (4.2)$$

$$- \frac{(A^2-B^2)^2 g_{\parallel}^2 g_{\perp}^2}{2H_o g^2 \beta^2 K^2 g^2}\,\sin^2\theta\cos^2\theta m_I^2$$

where $H_o = \frac{h\nu}{g\beta}$, $g^2 = g_{\parallel}^2\cos^2\theta + g_{\perp}^2\sin^2\theta$, and $K^2g^2 = A^2g_{\parallel}^2\cos^2\theta + B^2g_{\perp}^2\sin^2\theta$, being the angle between the Z-axis and the direction of the static magnetic field.

EXPERIMENTAL PROCEDURE

Single crystals of potassium dihydrogen phosphate with VO^{2+} impurity ions were grown from the aqueous solution of ANALAR grade KDP salt containing 1 percent vanadyl sulphate by weight. A good quality crystal was chosen and cut for EPR study. The dimensions of the cut crystal were 0.6x0.3x0.3 cm^3. The crystal was slightly blue in colour indicating the presence of VO^{2+} ion. The spectroscopic analysis of experimental crystal (carried out at the Spectroscopy Division, B.A.R.C., Bombay, India) revealed the presence of about 50 part per million of vanadium. The crystallographic axes of KDP were confirmed

by X-ray rotation picture taken with a Weisenberg camera.

The EPR spectrum was recorded on a Varian V-4502 spectrometer in the X-band, by mounting the crystal on a two plane goniometer crystal holder. Dual rectangular cavity was used and the spectra were recorded on a dual strip-chart recorder. The magnetic field was produced by a 12-inch electromagnet and was modulated by a 100 kHz modulator. DPPH, $g = 2.0036$, was used as a field marker. The frequency of the klystron was measured with a Hewlett Packard frequency meter X-532B.

RESULTS AND DISCUSSION

Two spectra corresponding to two different kinds of centres are obtained. One of them which is predominantly strong will be referred to as spectrum I while the other one which is of moderate intensity will be referred to as spectrum II. Fig. 4.2 shows the two spectra for H parallel to the c-axis of the crystal. Spectrum I shows an octet marked $A_1 \ldots A_8$ in the figure while spectrum II shows two octets marked $a_1 \ldots a_8$ and $b_1 \ldots b_8$. There is a remarkable similarity between the features of spectrum II and those of the spectra corresponding to the axial vanadyl pentahydrate complex $[VO(H_2O)_5]^{2+}$ observed by Manoogian and Mackinnon[1] and by Rao, Sastry and Venkateswarlu[2,9] in

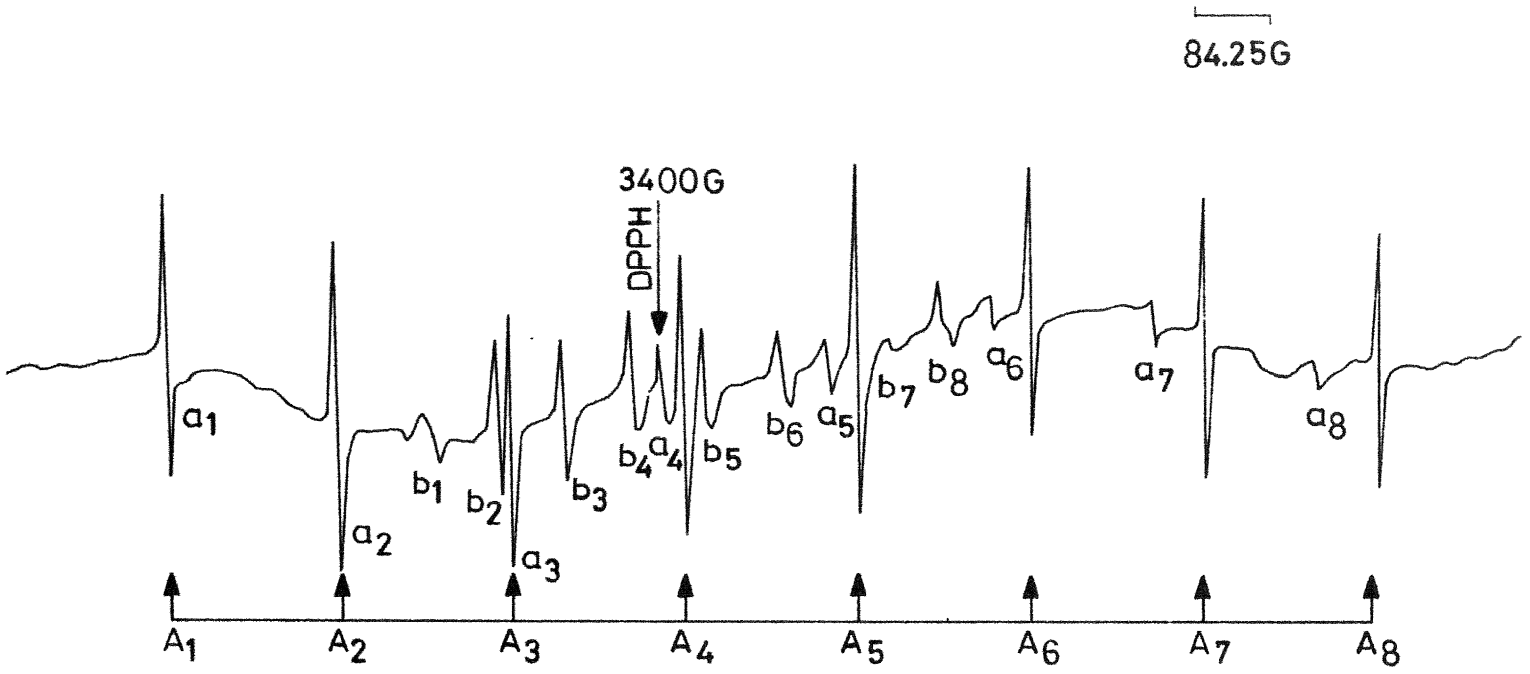

FIG. 4.2 THE ELECTRON PARAMAGNETIC RESONANCE SPECTRUM OF VO^{2+} ION IN KDP SINGLE CRYSTALS AT ROOM TEMPERATURE THE MAGNETIC FIELD BEING PARALLEL TO THE c-AXIS OF THE LATTICE. THE OCTET A_1 ..... A_8 BELONGS TO SPECTRUM I AND THE TWO OCTETS a_1 ..... a_8, AND b_1..... b_8 BELONGS TO SPECTRUM II.

different kinds of alums. The intensities of the octet $b_1....b_8$ are more than those of $a_1,....a_3$, the intensity ratio being nearly 2:1. The lines $a_1....a_8$ correspond to the VO^{2+} ions oriented along the c-axis of crystal while $b_1....b_8$ correspond to those perpendicular to the c-axis. In other words, $a_1....a_8$ may be called the parallel set (spectrum) (direction of VO^{2+} centres being parallel to H) while $b_1....b_8$ may be called the perpendicular set (spectrum). As the number of VO^{2+} centres will be twice for the perpendicular spectrum (X and Y direction) than those of parallel spectrum (Z-direction), the intensity of the perpendicular set is expected to be twice than that of the parallel spectrum. The X, Y and Z directions are the principal axes of the complex $[VO(H_2O)_5]^{2+}$ complex, the Z-direction approximately coincidin; with the c-axis of the crystal. Spectrum II has been analysed using the appropriate spin-Hamiltonian as that used by Manoogian et al[1] and Rao et al[2,9] [Eqs. (4.1) and (4.2). The constants obtained are given in Table 4.2 where the corresponding data of the complex in different alums are also listed for comparison.

Further, evidence for perpendicular and parallel sets for spectrum II comes from the splitting of perpendicular set into two when the direction of the

Table 4.2. Spin-Hamiltonian parameters for VO^{2+} doped in alum lattices and in the lattice of KDP. Hyperfine parameters are in units of 10^{-4} cm^{-1}.

Lattices	$g_{\parallel}$	$g_{\perp}$	A	B	References
RbAl alum	1.932	1.975	132.2	66.6	1
CsAl alum	1.932	1.979	133.4	65.7	1
KAl alum	1.936	1.977	177	68	2
NH_4Al alum	1.940	1.978	176	66	2
MAG alum	1.939	1.976	174	67	9
KDP (Spectrum I)	1.922	1.963	173.5	69.8	Present work
KDP (Spectrum II)	1.928	1.966	173.5	72	Present work

magnetic field is rotated by 10^{o} from the c-axis in the a c (b c) plane. A comparison of Fig. 4.3(a) and 4.3(b) taken with H parallel to c ($\theta = 0$) and $\theta = 10^{o}$ respectively, shows this splitting. The split components are marked b_1', b_1''; b_2', b_2'' etc., in Fig. 4.3 (b). b_1, b_2 etc., represent perpendicular set (spectrum) in Fig. 4.3(a). The parallel set (Fig. 4.3a) shows some structure and this becomes more clear when the direction of magnetic field becomes parallel to the a (b) axis (See Fig. 4.4). This indicates that the principal axes of the magnetic centres of this complex are not exactly parallel to the crystal axes, but are spread over a small angle about the crystal axes. However a more detailed study of spectrum II at different angles could not be taken up due to its overlap with the predominantly strong spectrum I for other orientation.

As mentioned earlier, spectrum I shows strong set of eight lines $A_1 \ldots A_8$ (Fig. 4.2) when H is parallel to the c-axis of the crystal. The angular variation of the spectrum and that of the hyperfine splitting in the a c (or b c) plane are shown in Figs. 4.5 and 4.6 respectively. When the rotation of the magnetic field is carried out in the a c (b c) plane (see Fig. 4.5) each hyperfine line of this set splits into a maximum of four components(Fig.4.3(b)).

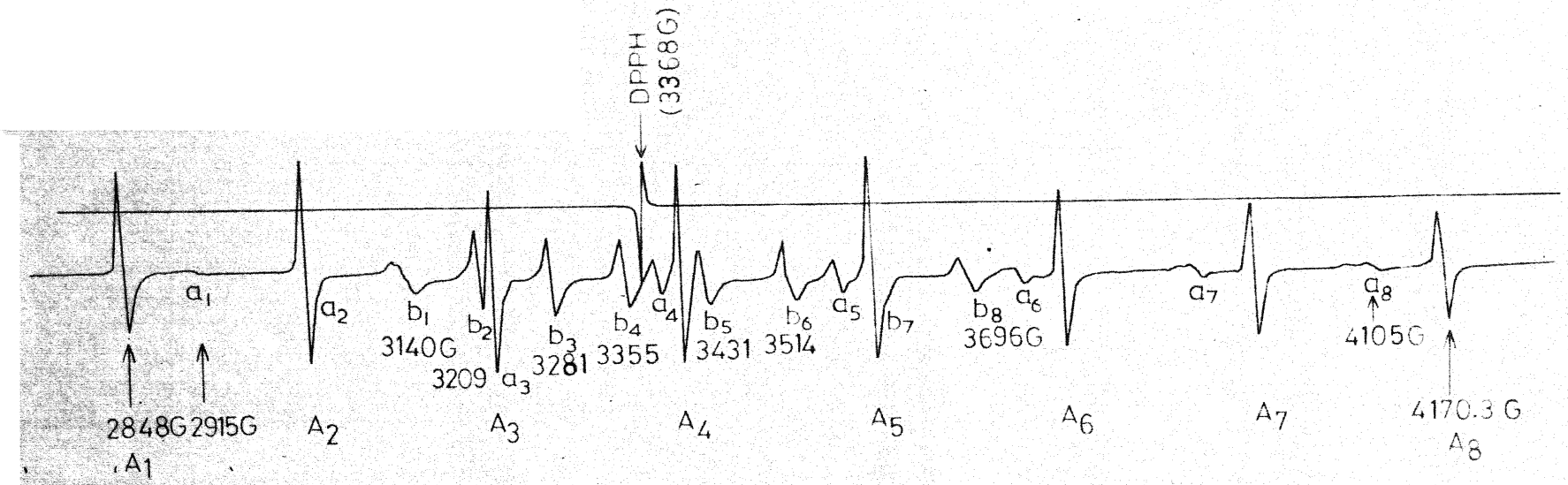

FIG. 4.3 (a) EPR SPECTRUM OF VO^{2+} ION IN KDP LATTICE AT ROOM TEMPERATURE WHEN THE MAGNETIC FIELD IS PARALLEL TO THE c-AXIS. THE PARALLEL SET $a_1 \ldots a_8$ SHOWN SOME STRUCTURE INDICATING THE SPREAD OF MAGNETIC AXES OVER SOME ANGLE AROUND c-AXIS. $A_1 \ldots A_8$ ARE HYPERFINE LINES OF SPECTRUM I. $a_1 \ldots a_8$ AND $b_1 \ldots b_8$ ARE PARALLEL AND PERPENDICULAR SETS OF HYPERFINE LINES OF SPECTRUM II.

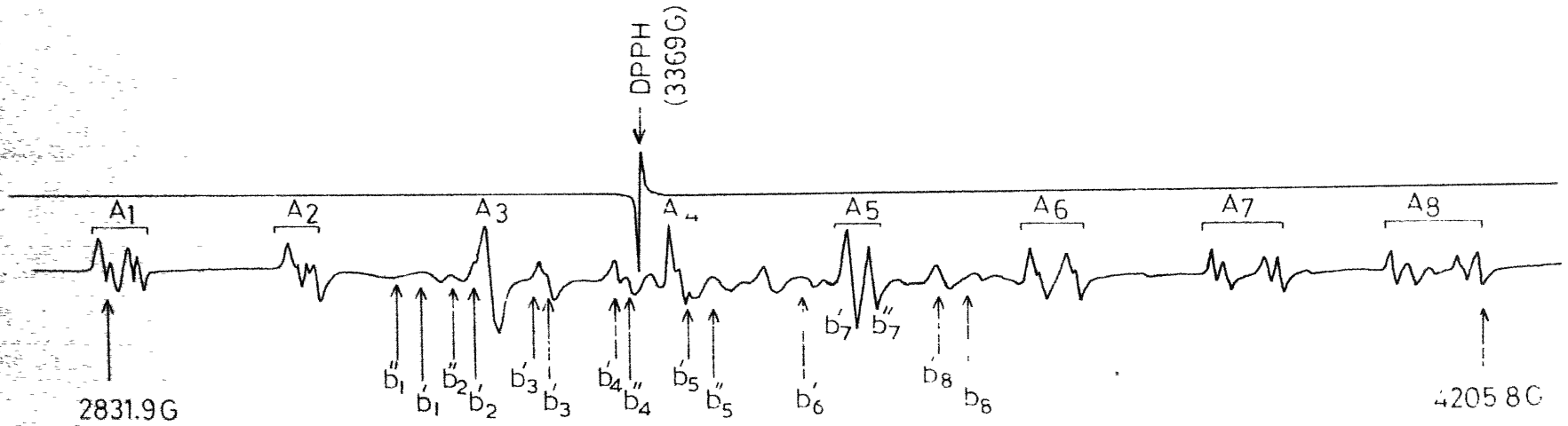

FIG. 4.3 (b) EPR SPECTRUM OF VO^{2+} ION IN KDP LATTICE AT ROOM TEMPERATURE WHEN THE MAGNETIC FIELD MAKES AN ANGLE 10^{0} WITH RESPECT TO THE b-AXIS IN THE ac (bc) PLANE. HYPERFINE LINES OF SPECTRUM I SPLITS INTO A MAXIMUM OF FOUR COMPONENTS. THE HYPERFINE LINES OF COMPLEX $[VO(H_2O)_5]^{2+}$ [FIG. 4.3(a)] SPLITS INTO TWO ONLY b_1',b_1''; b_2', b_2''; ETC. $A_1 \ldots A_8$ REPRESENT LINES OF SPECTRUM I AND b_1',b_1'' ..... b_8', b_8'' REPRESENT LINES OF SPECTRUM II.

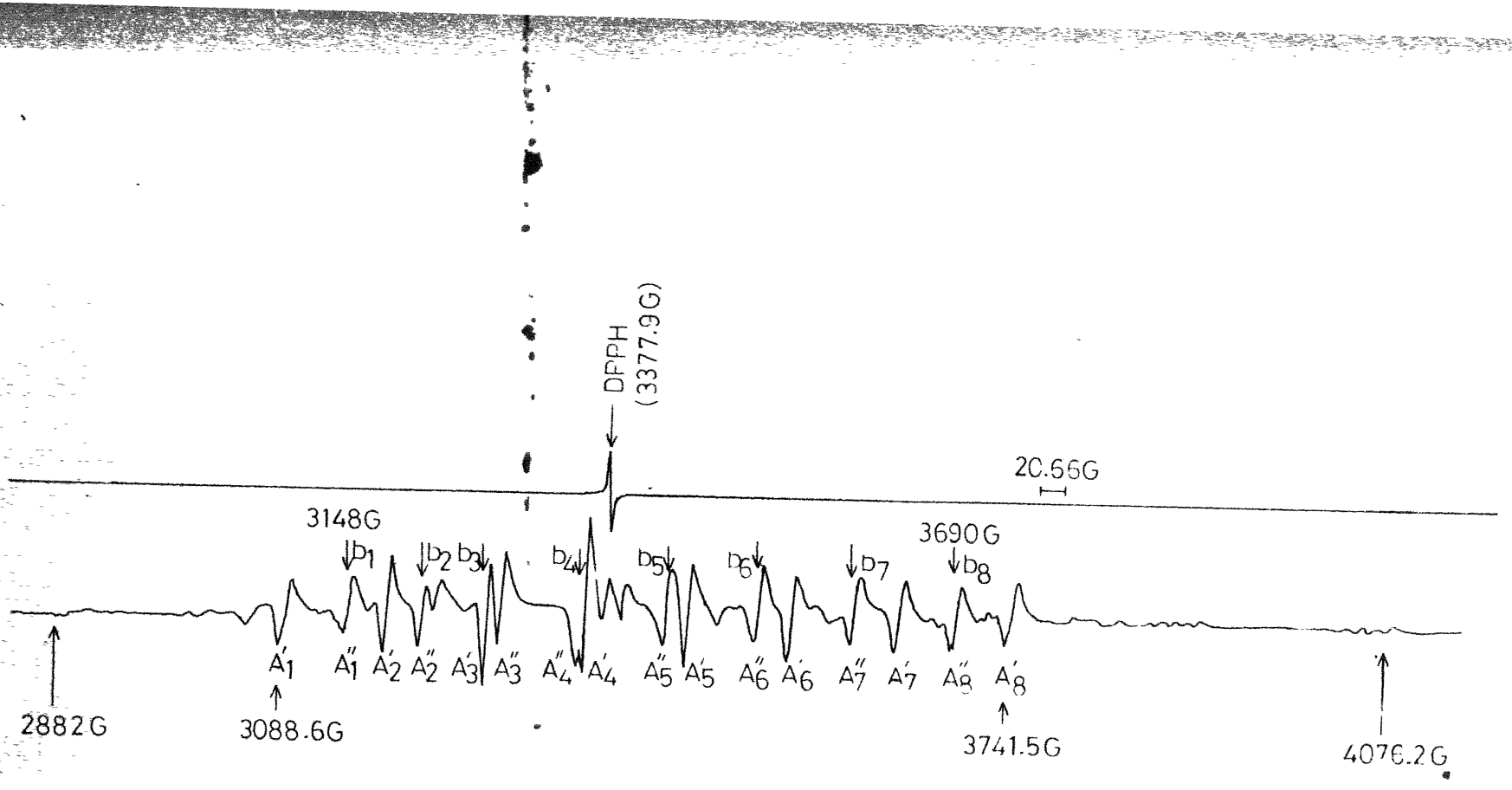

FIG. 4.4 EPR SPECTRUM OF VO^{2+} ION IN KDP LATTICE AT ROOM TEMPERATURE WHEN THE MAGNETIC FIELD IS PARALLEL TO a(b) AXIS. THE LINES MARKED A_1', A_2',.... A_8' AND A_1'',A_2''....A_8'' BELONG TO TWO SETS OF SITES WHICH BECOME INEQUIVALENT ALONG a(b) AXIS, BUT BECOME EQUIVALENT ALONG c-AXIS AND PRODUCE SPECTRUM I OF FIG.4.2 [4.3(a)]. THE LINES MARKED b_1, b_2.....b_3 CONSTITUTE PERPENDICULAR SET OF $[VO(H_2O)_5]^{2+}$ COMPLEX. PARALLEL SETS OF THE LATTER COMPLEX HAVE SEVERAL COMPONENTS.

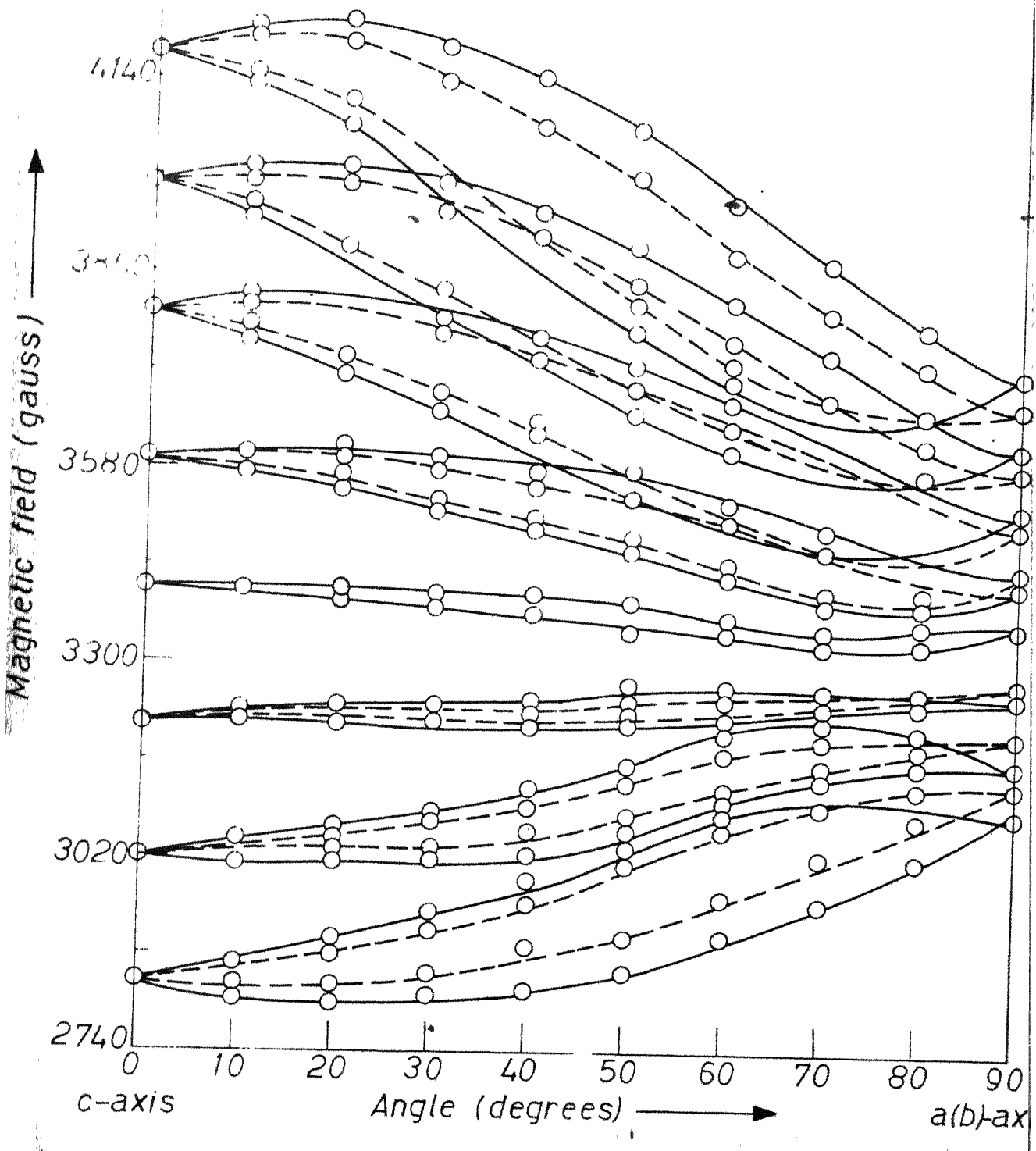

FIG. 4.5 ANGULAR VARIATION OF THE LINE POSITION OF VO^{2+} ION FOR SPECTRUM I, THE MAGNETIC FIELD BEING VARIED IN THE ac (bc) PLANE.

while it splits into two components only when the field is parallel to the a (b) axis. In an arbitrary direction each component further splits into two making a total of eight. The spectrum shows a maximum spread when H makes an angle of about 20° with the c-axis of crystal in the a b (b c)plane(see Figs. 4.5, 4.6 and 4.10). These observation suggests that the orientation of vanadyl complex formed is such that it has four pairs of symmetry-related sites with their Z-axes lying along the surface of a cone making an angle of about 20° with the crystallographic c-axis. Member of each pair are equivalent for orientation of the magnetic field in the ac(or bc) planes. Further two of the four pairs become one equivalent set while the other two form another equivalent set when the magnetic field is along the a (or b) axis. All the four pairs becomes equivalent when the magnetic field is parallel to the c axis.

The observation suggest further that the Z-axis is in the ac (or bc) plane making an angle of about 20° with the c-axis. This behaviour can be explained if one assumes that VO^{2+} enters the lattice at an interestitial site where the position of four oxygens is congenial for the formation of a nearly square pyramidal vanadyl complex in which vanadyl is known to exist such as in vanadyl acetyl acetonate.[11] The structure of vanadyl acetyl acetonate is shown in Fig. 4.7, for illustration. The projection

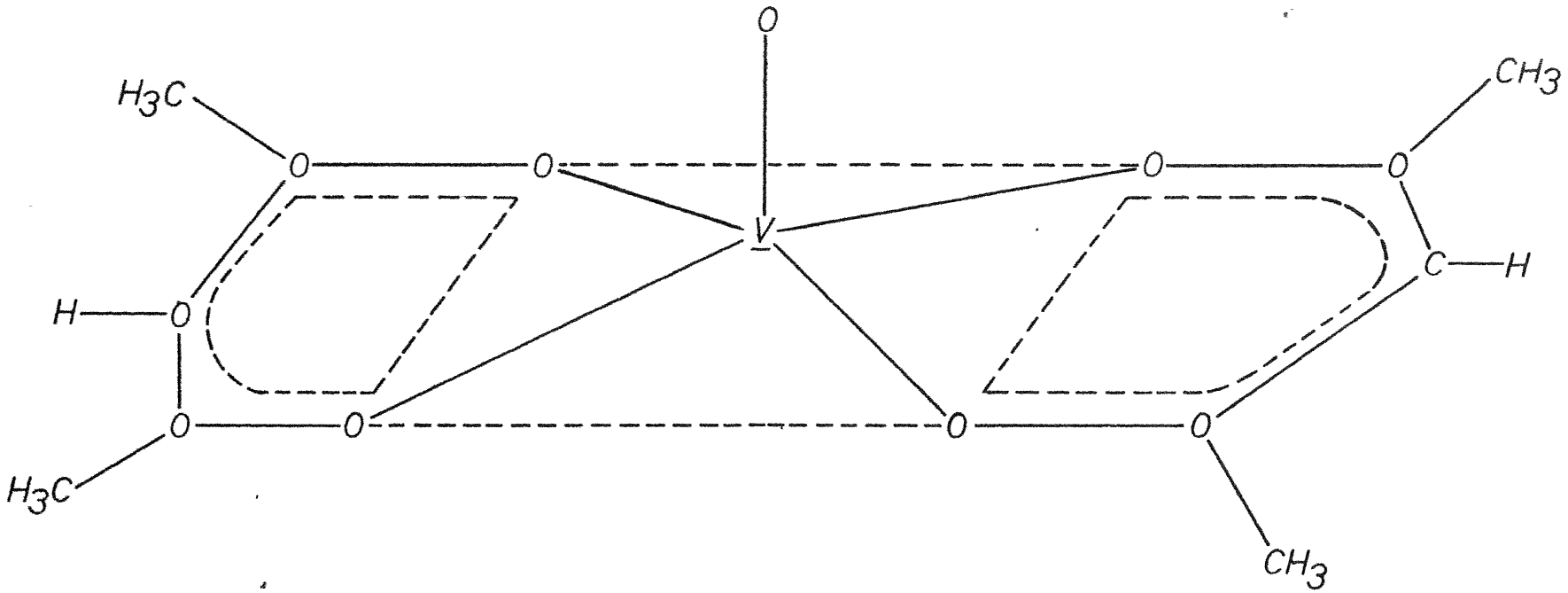

FIG. 4.7 STRUCTURE OF [illegible] (R. [illegible] ADVANCED INORGANIC CHEMISTRY, 2nd Ed., p. [illegible] 1963).

of KH_2PO_4 in the ab plane (Fig. 4.8) shows four oxygens, numbered 1,2,3,4 lying nearly in a plane with its normal making an angle of about 40° with the c-axis. However, when VO^{2+} ion enters the lattice forming a complex with these oxygens, the complex seems to get stabilized such that V = O bond makes an angle of 20° with the c-axis as observed. The positions of the four oxygen atoms more likely form a rectangle making the complex a non axial one. Thus the rhombic components may probably be responsible for the observed doubling of the lines, making them eight, when the crystal is rotated such that the magnetic field is out of the ab plane. A model of the orientation of Z-axis is shown in Fig. 4.9. The spectrum has been analysed using the expressions given in equation (4.2) appropriate to axial symmetry and the parameters obtained are given below:

$$g_{\parallel} = 1.922 \pm .001$$
$$g_{\perp} = 1.963 \pm .001$$
$$A = (178.5 \pm 2.5) \times 10^{-4} cm^{-1}$$
$$B = (69.3 \pm 3) \times 10^{-4} cm^{-1}$$

The angular dependence of hyperfine constants is shown in Fig. 4.10. The points are experimental points and the curve is a theoretical one, calculated using the

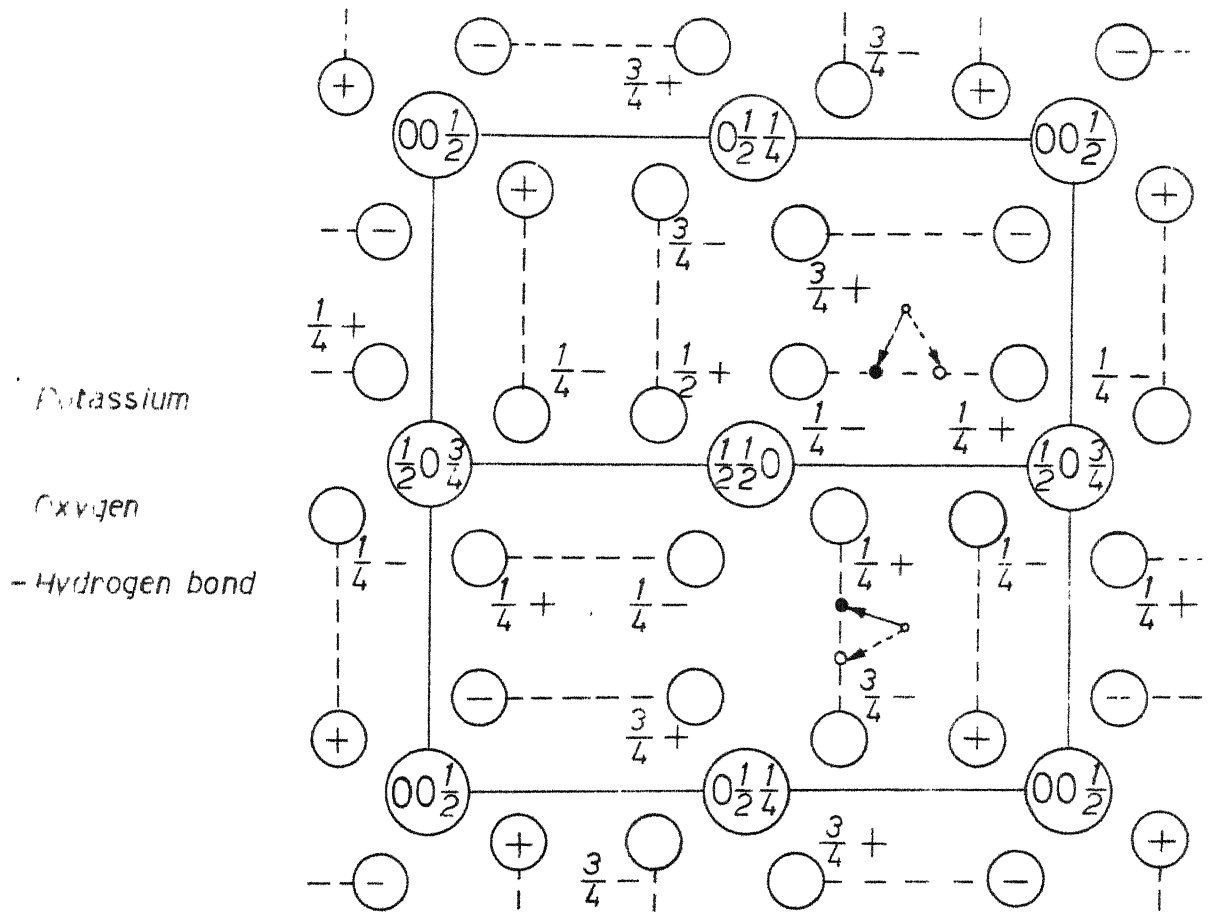

FIG. 4.1 SCHEMATIC PROJECTION OF TETRAGONAL KH_2PO_4 C.. (001). THE POSITIONS OF PHOSPHORUS ARE AT POTASSIUM 3/2 ABOVE AND BELOW THE POTASSIUM (OF SHOWN). THE ARROWS SHOW THE PROJECTIONS OF THE DIRECTIONS ALONG WHICH THE VO^{2+} IONS MIGHT SIT ALI.. L.

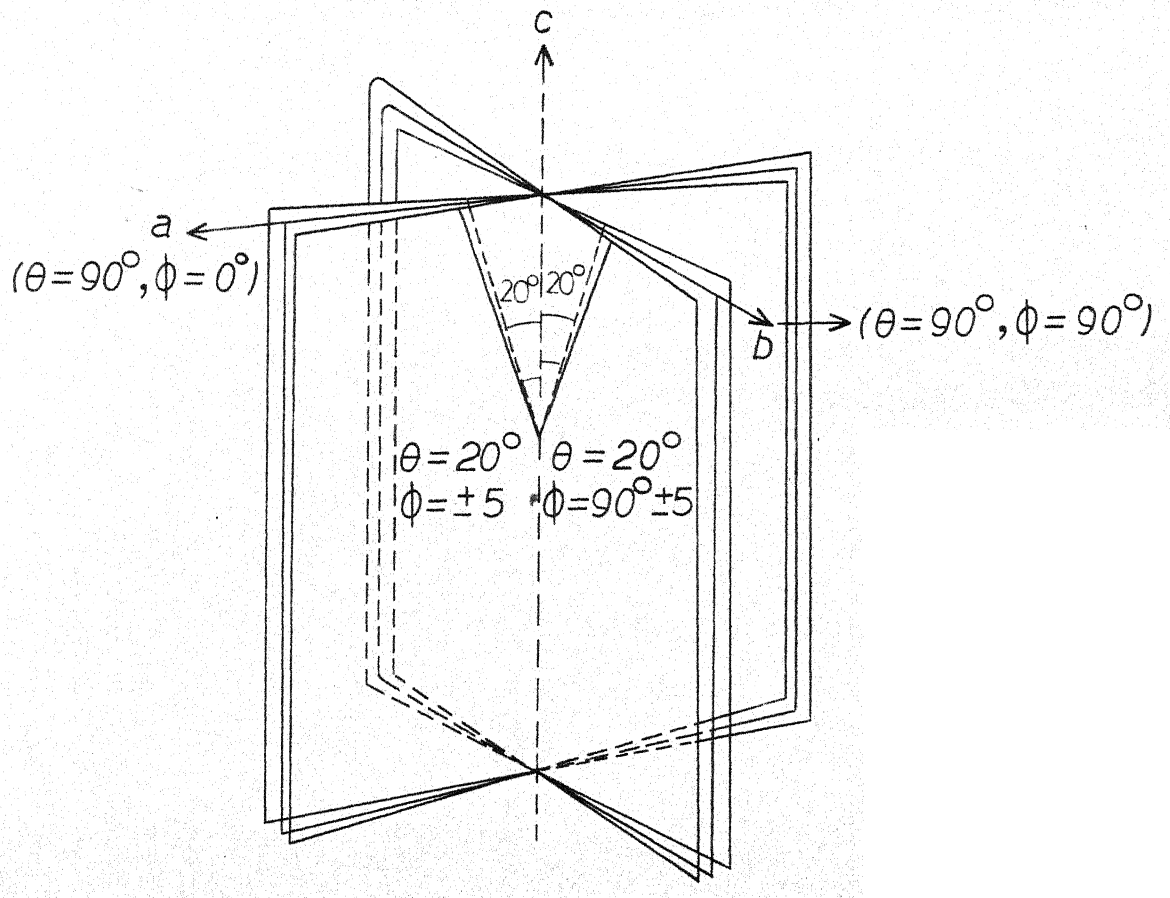

FIG. 4.9 SCHEMATIC REPRESENTATION OF TWO PAIRS OF Z-AXIS OF VO^{2+} ION PARTLY RESPONSIBLE FOR DOMINANT SITE. FOR THE CLARITY OTHER TWO PAIRS ARE NOT SHOWN.

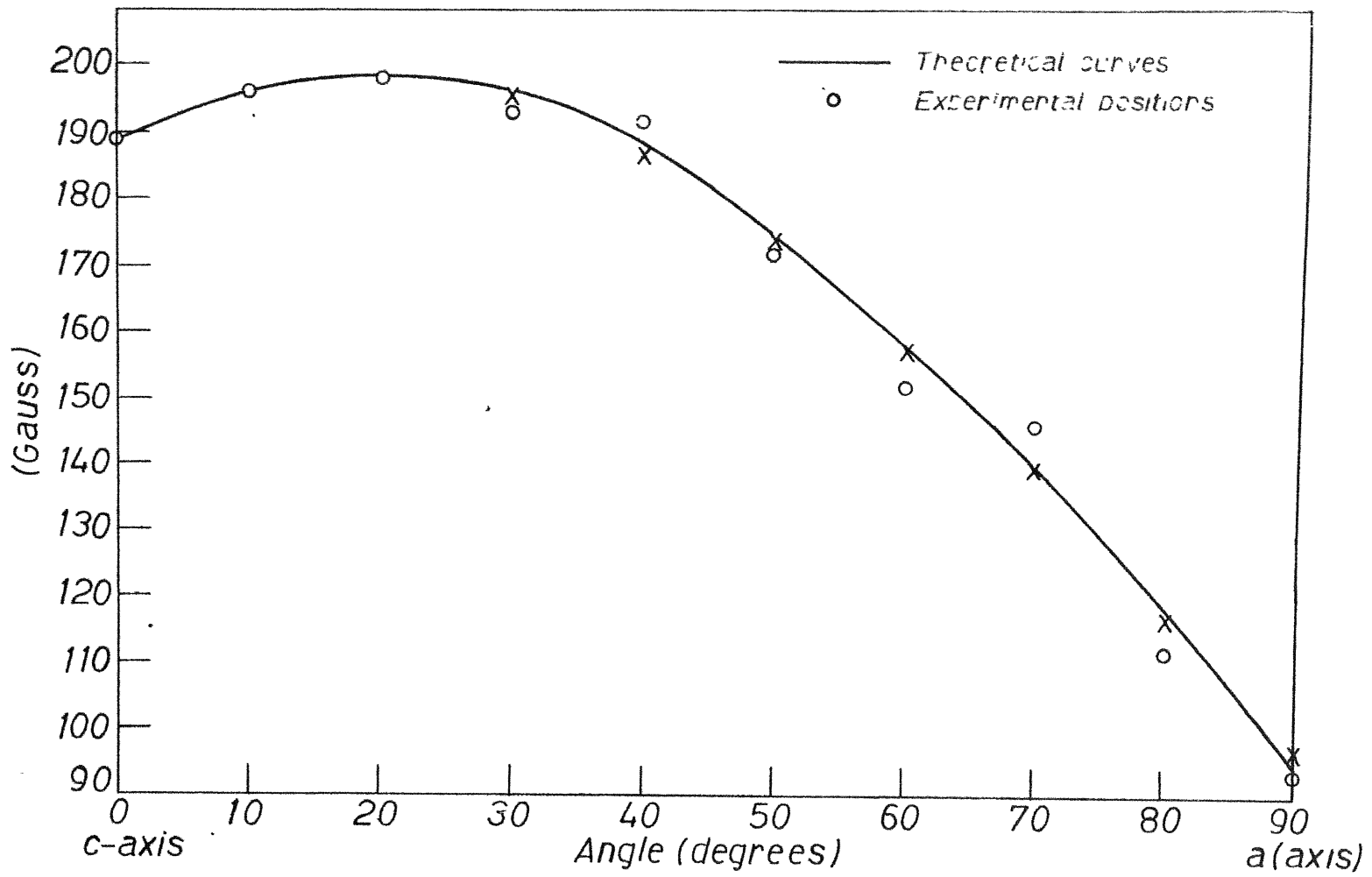

FIG. 4.10 EXPERIMENTAL AND THEORETICAL PLOTS OF [illegible] θ (SEE TEXT) IN THE ac PLANE. [illegible] θ IS MEASURED WITH RESPECT TO THE c AXIS AND $A = (A_{//}^2 A_{//}^2 \cos^2\theta + A_{\perp}^2 A_{\perp}^2 \sin^2\theta)^{\frac{1}{4}}$.

constants given above and the expression (4.2). It may be mentioned that B and $g_{\perp}$ values are somewhat approximate in view of the observed non axial nature of complex.

In conclusion, it may be mentioned that in most of the investigations of VO^{2+} in variety of lattices reported in literature show that VO^{2+} does not enter the lattice as a point defect but it forms a complex, the formation of which is helped and stabilized by the structure of the host lattice. It is well known that vanadyl ion exists as $[VO(H_2O)_5]^{2+}$ complex in water solutions and in a number of hydrated salts such as vanadyl sulphate. It is probably the most well understood complex involving the vanadyl ion. However, it is interesting to note the formation of this complex in KDP single crystal. Ordered intercrystallization of two different types of structures is well know and it has recently been reported by Sastry[10] in the EPR study of Pd doped NH_4Cl single crystal. Thus, during the process of crystallization of KDP from water solution containing the VO^{2+} impurity, $[VO(H_2O)_5]^{2+}$ complex gets probably, trapped in the crystal and there is an ordered intercrystallization of this complex, though small in concentration, in KDP crystal.

REFERENCES

1. A. Manoogian and J. MacKinnon, Can. J. Phys. 45, 2769 (1967).

2. K. V. S. Rao, M. D. Sastry and P. Venkateswarlu, J. Chem. Phys. 49, 4984 (1968).

3. R. H. Borcherts and C. Kikuchi, J. Chem. Phys. 40, 2270 (1964).

4. H. J. Gerritsen and R. H. Lewis, Phys. Rev. 119, 1010 (1960).

5. I. Siegel, Phys. Rev. 134, 193 (1964).

5a. S. K. Banerjee, Ph.D. Thesis, Indian Institute of Technology, Kanpur, India (1969).

6. J. West, Z. Krist, 74, 306 (1930).

7. C. S. Ballhausen, H. B. Gray, Inorg. Chem. 1, 111 (1962).

8. B. Bleaney, Phil. Mag. 42, 441 (1951).

9. K. V. S. Rao, M. D. Sastry and P. Venkateswarlu, J. Chem. Phys. 51, 812 (1969).

10. M. D. Sastry, J. Chem. Phys. 64, 3957 (1976)

11. F. A. Cotton and G. Wilkinson, 'Advances in Inorganic Chemistry', , 2nd. Ed. P. 815, Interscience Publishers (1968).

CHAPTER 5

ELECTRON PARAMAGNETIC RESONANCE OF Cr^{3+} ION IN $TlAl(SO_4)_2 \cdot 12\,H_2O$ SINGLE CRYSTAL

ABSTRACT

The electron paramagnetic resonance of Cr^{3+} ion in $TlAl(SO_4)_2 \cdot 12H_2O$ single crystals has been studied at room temperature. Cr^{3+} impurity ion seems to have replaced Al^{3+} ion in the crystal lattice. Four directionally different, otherwise, similar magnetic centers are found. The site symmetry at Cr^{3+} has been found to be trigonal with the principal Z axis along crystallographic <111> axis. Using the spin Hamiltonian appropriate to trigonal symmetr relevant parameters have been calculated.

INTRODUCTION

The study of electron paramagnetic resonance of Cr^{3+} ions with varied concentrations in single crystals of alums has drawn considerable attention. The work of Bagguley and Griffiths[1] on K, Rb, Cs, NH_4 and NH_3CH_3 chromic sulphate alums at room temperature reveals the existence of four magnetically non-equivalent, otherwise similar, complexes subjected to a small trigonally distorted octahedral crystal field. Further, the work of Danilov and Manoogian[2] and that of Manoogian and Danilov[3] in similar host lattices but containing Cr^{3+} in diluted amount demonstrates similar magnetic centers in trigonally distorted crystal field of octahedral symmetry. The present chapter describes the result of an EPR study of Cr^{3+} ion in $TlAl(SO_4)_2.12H_2O$ single crystals. It may be mentioned that the work of Manoogian and Leclerc[4] on the temperature variation of the D parameter in Cr^{3+} doped alums appeared after the present work was completed. However, they have reported only the D value for Cr^{3+} in TlAl sulphate alum at 77°K, 195°K and 297°K and no other details of the EPR work on this system are given.

THE STRUCTURE OF ALUMS

The alums are a series of double salts for which the general formula may be expressed as $M^IM^{II}(RO_4)_2.12H_2O$, in which M^I and M^{II} are monovalent and trivalent cations respectively and R stands for sulphur,

selenium or tellurium.[5] The structure and classification of alums have been studied by Lipson and Beevers[6] and Lipson.[7] The crystals belong to a cubic system and possess point group symmetry $T_h = (2/m)\bar{3}$ and space group T_h^6 (Pa 3).[8] There are four molecules in the unit cell. The nearest neighbours of monovalent and trivalent cations are six water molecules and they constitute octahedrons. The octahedron about the monovalent cation is somewhat distorted whereas the one about the trivalent cation is nearly regular.

The alums are classified as α, β or γ depending on the differences in the arrangement of atoms, molecules or ions. In the α type alums, the <111> axes of the water octahedron surrounding the trivalent cation coincide with the <111> axes of the crystal, but the cubic axes of water octahedron are displaced from the cubic axes of crystal by a rotation of 9.5° about the <111> direction of the crystal. There is a small trigonal distortion along the crystallographic <111> direction. The angle of rotation in the β type alum is 0° and in the γ type alum it is about 40°.[3] For the γ type alum the sulphate groups are oriented in opposite directions along the crystallographic body diagonal.

Lipson[7] postulated that the size of the monovalent cation determines the type of alums. A medium

size cation is responsible for α type alum, larger size for β type alum and small size for γ type alum. Though the mass number of Tl is high the ionic radius of Tl^+ is equal[9] to that of Rb^+. Thus TlAl alum belongs to α type alum.[10] The size of the trivalent cation also determines the type of alum.[11-13] The edge of its unit cell is 12.232Å.[14]

EXPERIMENTAL PROCEDURE

Single crystals of thallium aluminium alum doped with Cr^{3+} ions were grown at room temperature by slow evaporation of the aqueous solution of thallium sulphate and aluminium sulphate taken in stoichiometric ratio containing small amount of chromic sulphate. The crystals were found to grow with well defined (111) planes in the usual habit of other alums.[15] The crystal taken for the EPR study was transparent and colourless with 0.7x0.6x0.3 cm^3 dimension.

The electron paramagnetic resonance spectrum was recorded on a Varian V-4502 X-band spectrometer using a cylindrical cavity, a 12 inch electromagnet and 100 kHz modulation. The frequency of klystron was measured with a Hewlett-Packard frequency meter X-532 B. DPPH, for which $g = 2.0036$, was used as field marker.

THEORY

Cr^{3+} ion has a $3d^3$ configuration and its ground state is ^4F. This state has a seven-fold orbital degeneracy and a four-fold spin degeneracy. In the presence of a crystalline field of octahedral symmetry the orbital degeneracy is partially lifted and the resulting orbital states are a singlet Γ_2 state and triply degenerate Γ_4 and Γ_5 states. The triply degenerate states lie several thousand wave numbers above the Γ_2 state. The state of our interest is Γ_2 which has four-fold spin degeneracy. This spin degeneracy cannot be lifted by spin orbit coupling alone. In the presence of small axial distortion, the four-fold spin degeneracy is partially removed leaving two Kramers' doublets. Further, the application of magnetic field can remove the degeneracy of the Kramers' doublets. That is shown in Fig. 5.1. All the Zeeman components belonging to Γ_2 state are appreciably populated at room temperature as per the Boltzman's distribution law. The energy gaps at moderate fields are comparable to the microwave frequency used. Therefore, three absorption signals for transition between these states under the selection rule $\Delta M_s = \pm 1$ can be observed. Here, M_s takes values +3/2, +1/2, -1/2, and -3/2. The spectrum, so obtained, constitutes fine structure. A further splitting of fine structure can

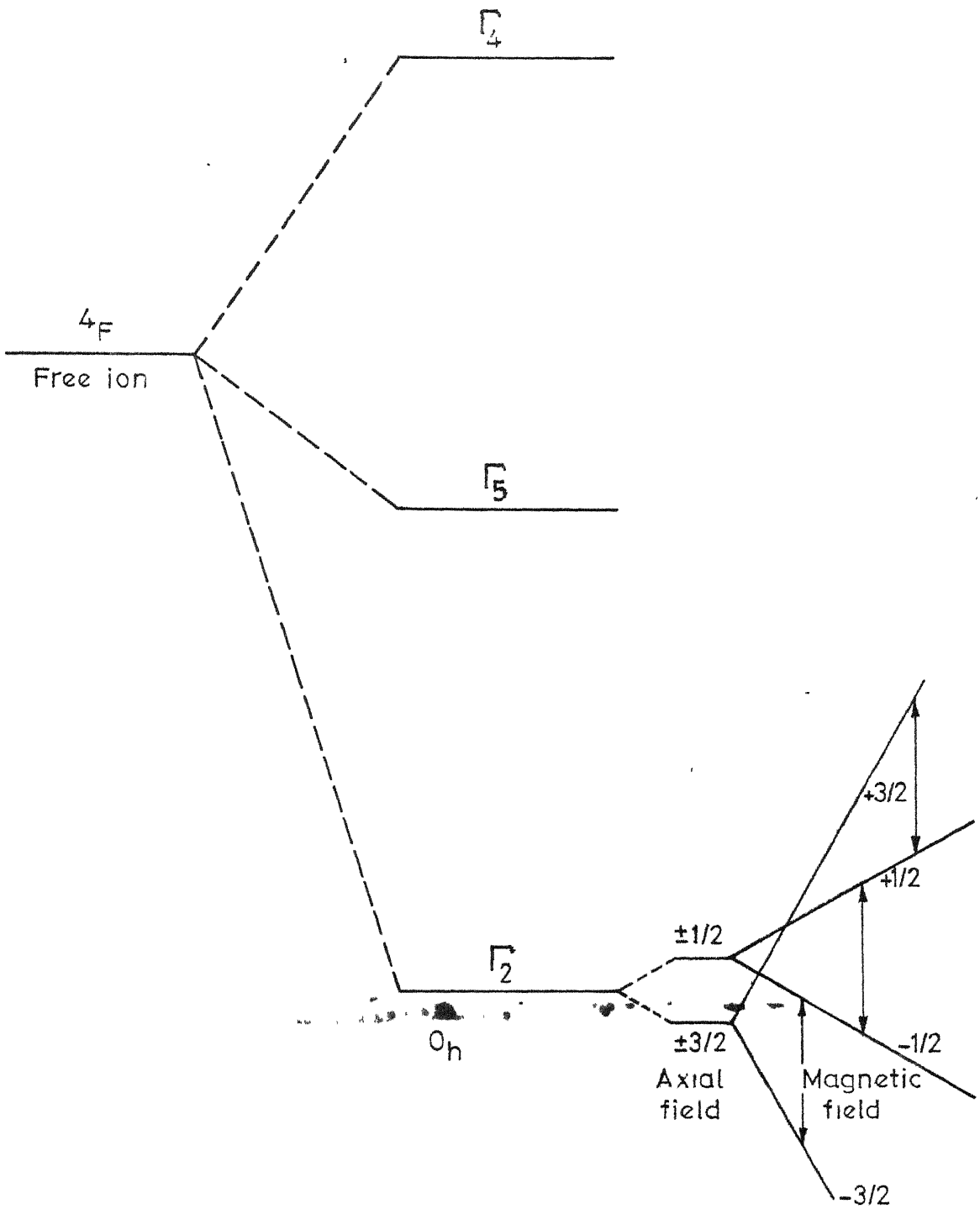

Fig.5.1 Energy level diagram of Cr^{3+} in an octahedral -plus-trigonal symmetry, the zero field splitting gives two kramers' doublets. EPR transitions $\Delta M_S = \pm 1$ between Zeeman levels are indicated by arrows.

result if the nucleus has a nonvanishing spin. There are two main isotopes of chromium. ^{52}Cr (I = 0) has natural abundance of 84 percent and ^{53}Cr (I = 3/2) of 9.5 percent. The isotope ^{53}Cr (I = 3/2) is expected to give hyperfine splitting. However, in the present study no hyperfine splitting was observed. This might be due to weak intensity and close splitting of the hyperfine components which seem to have been masked by the fine structure line of the more abundant ^{52}Cr.

The appropriate spin Hamiltonian for Cr^{3+} ion in a trigonally distorted octahedral field of host lattice, subjected to a external magnetic field is given[2] below:

$$\mathcal{H} = g_{\parallel} \beta H_z S_z + g_{\perp} \beta (H_x S_x + H_y S_y) + D[S_z^2 - (1/3)S(S+1)]$$

If the magnetic field is oriented parallel to the Z-direction, then

$\mathcal{H} = g_{\parallel} \beta H_z S_z + D[S_z^2 - (1/3) S(S+1)]$. The eigenstates are $|\pm 3/2\rangle$ and $|\pm 1/2\rangle$. The eigen values of the above Hamiltonian are

$$\pm 3/2\ g_{\parallel}\ \beta\ H + D,\ \pm 1/2\ g_{\parallel}\ \beta\ H - D$$

The field positions of various transition under the selection rule $\Delta M_s = \pm 1$, are given below:

$$H_1 = H_o - 2D$$
$$H_2 = H_o$$
$$H_3 = H_o + 2D$$

where D is expressed in gauss and H_o stands for $\frac{h\nu}{g_{\parallel}\beta}$.

RESULTS AND DISCUSSION

The EPR spectrum of Cr^{3+} ion in a single crystal of $TlAl(SO_4)_2.12H_2O$ was recorded at room temperature and its angular variation has been studied in the crystallographic (110) and (111) planes and is shown in Figs.5.2 and 5.3 respectively. The planes of the crystal were identified from the usual growth habits and morphology of alums.[15] The angular variation of line positions is quite similar to those obtained by Bullow and Manoogian[2] in RbAl and CsAl alums. It is found that there are four similar but directionally different magnetic complexes for Cr^{3+} ion in TlAl alums, each being responsible for three EPR transitions under the selection rule $\Delta M_s = \pm 1$. Transitions from four complexes are identified with H in (111) plane and are marked I, II, III and IV and are shown in Fig. 5.3. There are, some more lines of weak intensity towards the low field side. These lines seem

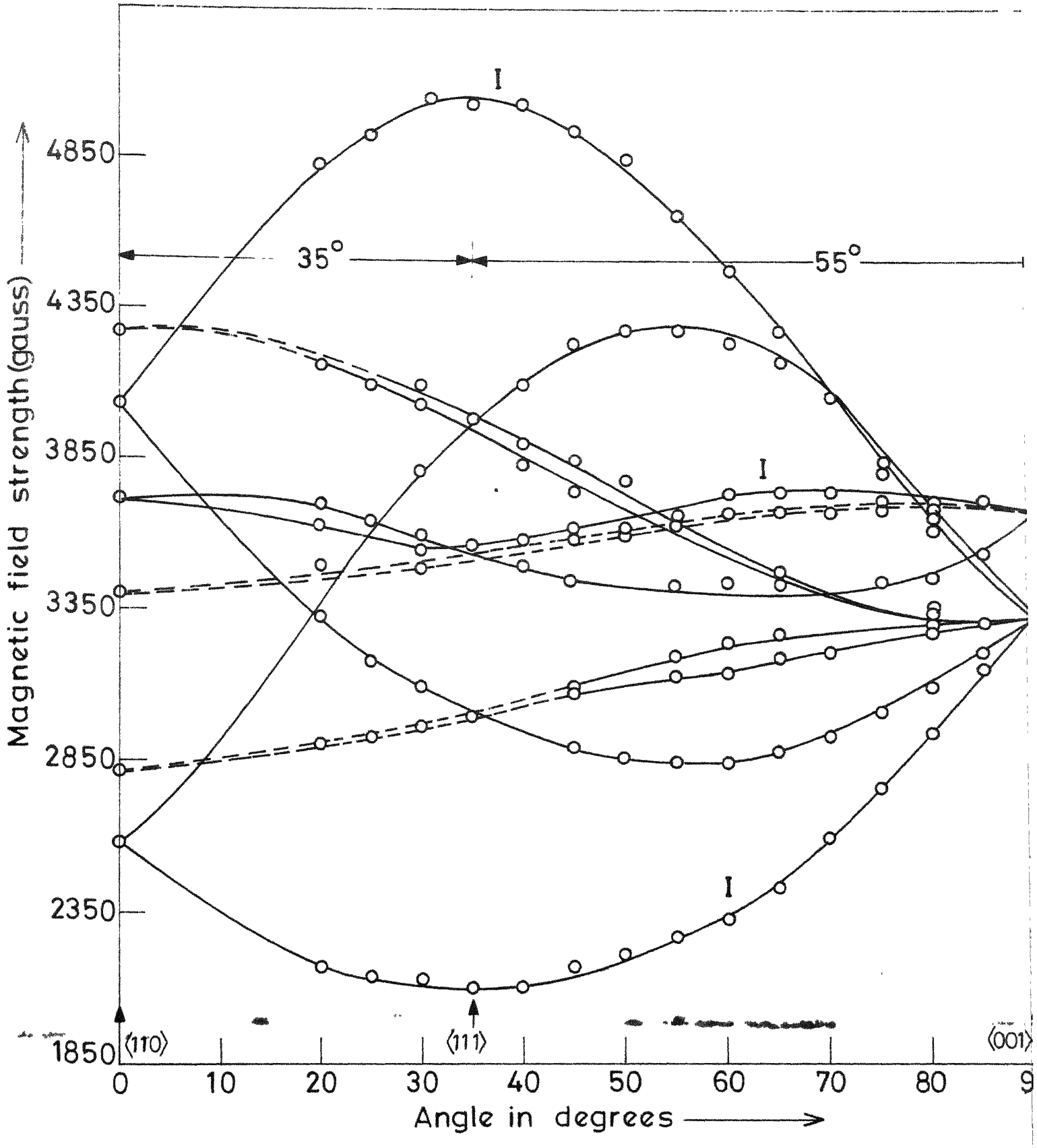

FIG. 5.2 THE ANGULAR VARIATION OF THE EPR LINE OF Cr^{3+} ION WHEN THE CRYSTAL IS ROTATED ABOUT <110> DIRECTION AT ROOM TEMPERATURE.

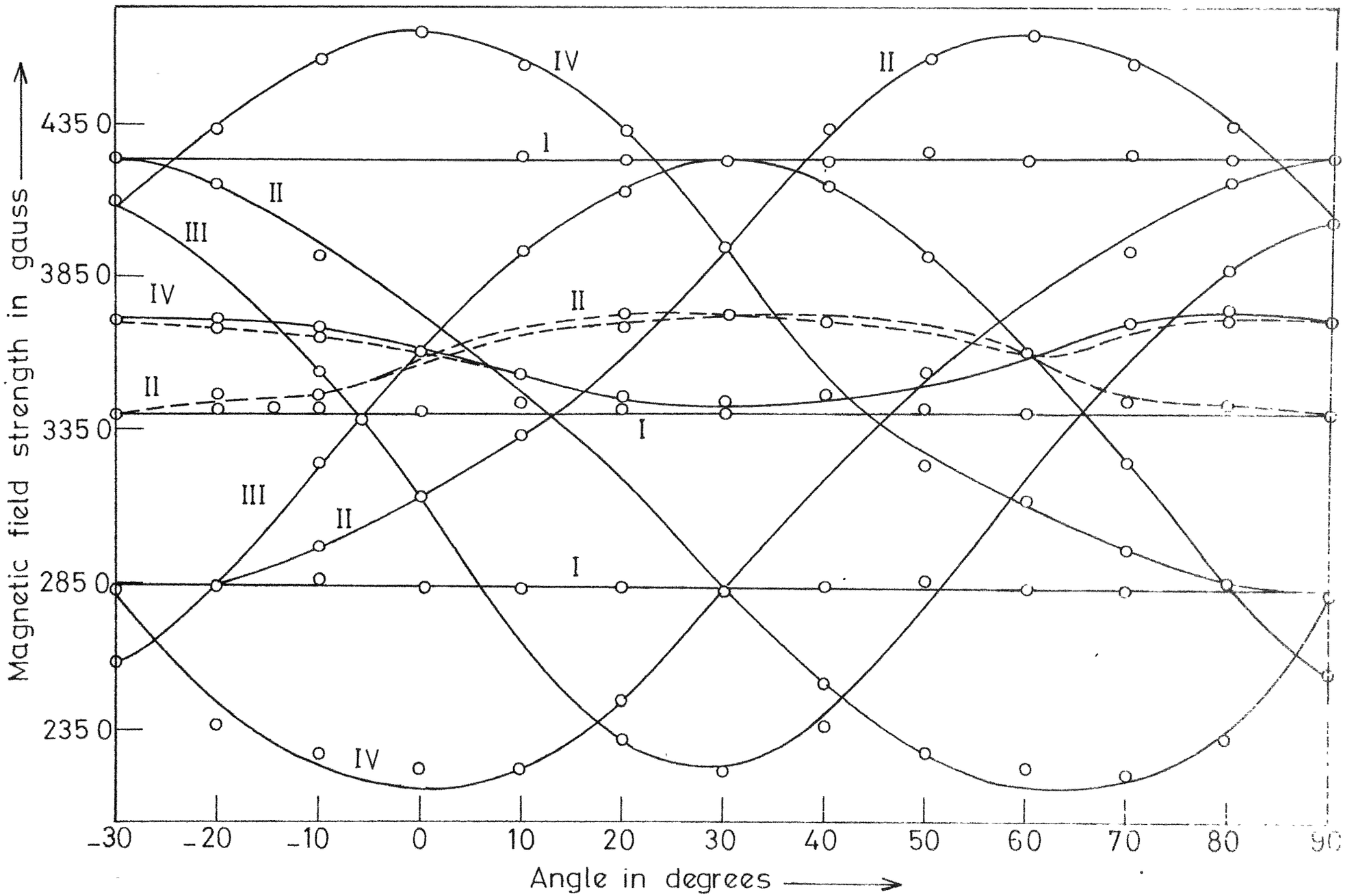

Fig. 5.5 ANGULAR VARI[illegible] (Δ)
[illegible]

to be forbidden ones. When the angular variation of the magnetic field was done in the (110) plane of the crystal lattice, the spectrum had shown a maximum spread with magnetic field along the <111> direction. This spectrum is shown in Fig. 5.4. It is in qualitative agreement with that of Cr^{3+} ion in ammonium chromium alum.[16] The spectrum coalesces when the magnetic field is parallel to the <100> direction. This is in agreement with the expected $(3\cos^2\theta - 1)$ type variation, indicating that Cr^{3+} ion is at an axially distorted site in the lattice.

The angular variation of the spectrum in the (111) plane of crystal lattice revealed perfect 60° repetition of the EPR spectra as in Cr^{3+} doped gallium alum.[2] This is in conformity with the existence of C_3 symmetry in the system and it appears that the structure of the TlAl alum is also cubic with some local distortion about the <111> direction, making the local symmetry a trigonal one. From the angular variation in the (111) plane (see Fig. 5.3) it is clear that there is a set of three lines which is angular independent. The separation between the extreme lines of this set is nearly half the separation between the extreme lines (parallel spectra) obtained when H is parallel to <111> direction. This means that this angular independent set is the perpendicular (X/Y) spectrum. From the parallel and the

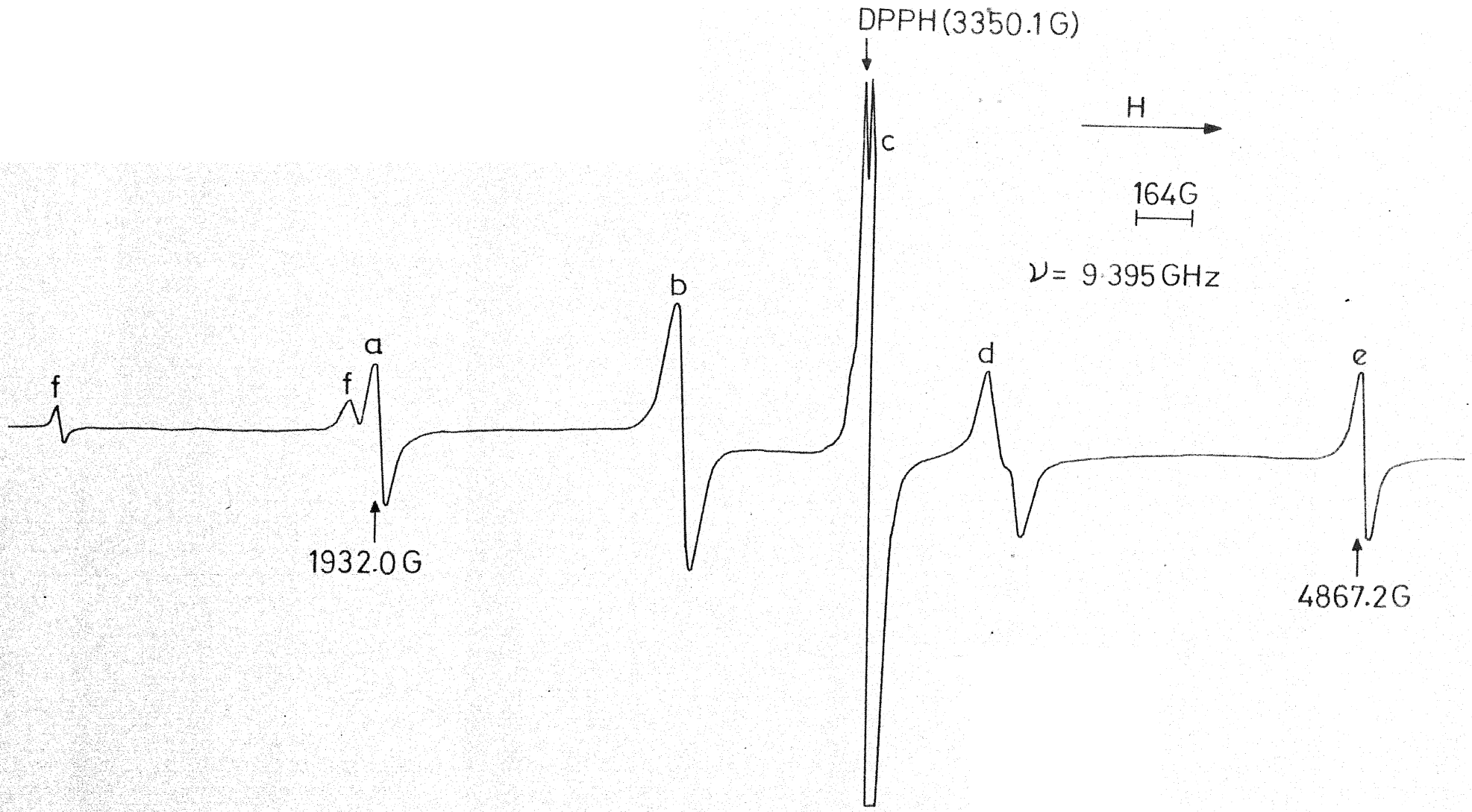

FIG. 5.4 EPR SPECTRUM OF Cr^{3+} ION IN $TlAl(SO_4)_2.12H_2O$ AT ROOM TEMPERATURE WHEN THE STATIC FIELD H IS PARALLEL <111> DIRECTION. THE LINES b AND d ARE TRIPLY DEGENERATE, c QUADRUPLY DEGENERATE WHEREAS a and e ARE SINGLE LINES. THE LINES a, c AND e CONSTITUTING Z-AXIS SPECTRUM OF ONE OF THE MAGNETIC CENTRE. THE LINES MARKED f SEEM TO BE FORBIDDEN.

perpendicular spectra the $g_{\parallel}$, $g_{\perp}$ and D values have been calculated. The values are given below

$$g_{\parallel} = 1.976 \pm .004, \quad g_{\perp} = 1.972 \pm 0.004$$

$$D = (679 \pm 5) \times 10^{-4} \text{ cm}^{-1}$$

The experimental and theoretical angular variation of the fine structure of Cr^{3+} ion at one of its sites in $TlAl(SO_4)_2.12H_2O$ is shown in Fig. 5.5. The theoretical expressions[13] for the fine structure line positions are used after appropriate modification.

The temperature variation of D parameter of Cr^{3+} ions in a series of hydrated salts reported by Manoogian et al[4] shows that in the case of TlAl alum its value is $683 \pm 5 \times 10^{-4}$ cm^{-1} at room temperature, which is close to $(679 \pm 5) \times 10^{-4}$ cm^{-1}, from the present experiment.

The origin of trigonal distortion is probably due to the effect of ligand around the magnetic ion.[22] In α type alums, keeping trivalent cation to be the same, we can correlate to some extend as shown in Table 5.1 the ionic radii of monovalent cations with the magnitude of the D parameter of the Cr^{3+} ion. This table shows that the value of the D parameter increases with the increase of ionic radius of the monovalent

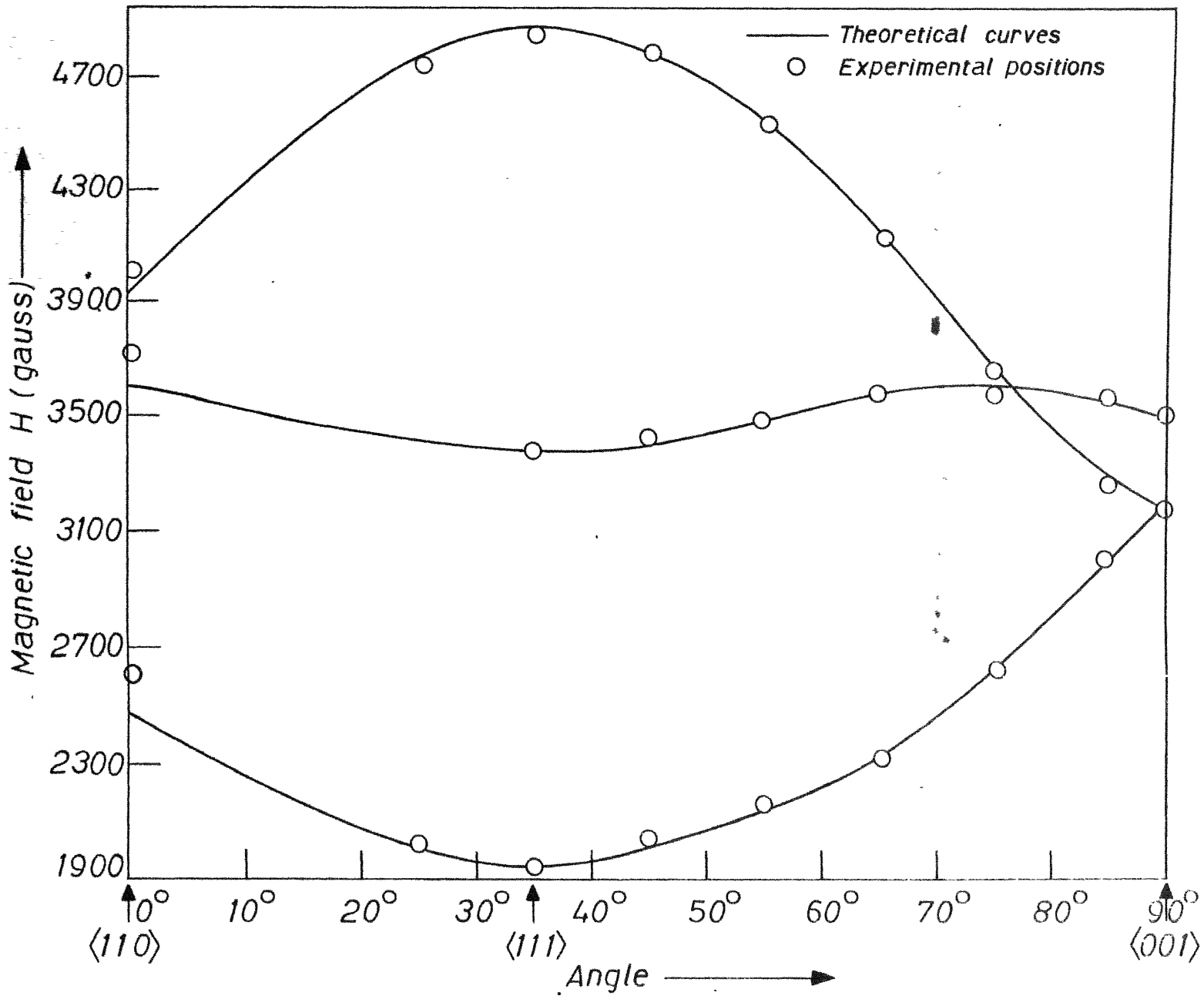

FIG. 5.5 ANGULAR VARIATION [illegible] Mn^{3+} [illegible]

Table 5.1 A comparison of ionic radii and D parameters for some alums.

α-Alums	Ionic radius of monovalent cation[2] Å	D (10^{-4} cm^{-1})	Edge of unit cell[5] Å
KAl alum	1.33	460[1]	12.14
NH_4Al alum	1.43	500[1]	12.18
NH_4Al alum		435[4]	
RbAl alum	1.47	531±5[4]	
TlAl alum	1.47	635±5[4]	12.21
TlAl alum	1.47	679±5 (Present work)	12.21

cation. It thus looks plausible as pointed out by Danilov and Manoogian[2] from other considerations that the size determines the distortion of the six water molecules coordinated to it and also the distribution of the sulphate groups. The displacements of these water molecules and sulphate groups might influence the formation of trigonal distortion at the trivalent site of the magnetic ion.

REFERENCES

1. D. . . S. Ba. dley and J. . . E. Griffiths, Proc. Roy. Soc. (London) A204, 188 (1950).

2. A. G. Damilo and A. Lanco ian, Phys. Rev. B6, 4097 (1972).

3. A. L. oo.ian and A. G. Damilov, Can. J. Phys. 48, 1448 (1970).

4. A. Lancoqian and A. Declere, J. Chem. Phys. 63, 4450 (1975).

5. J. . . Cork, Phil. Mag. 4, 683 (1927).

6. H. Lipson and C. A. Beevers, Proc. Roy. Soc. (London) A148, 664 (1935).

7. H. Lipson, Proc. Roy. Soc. (London) A151, 347 (1935).

8. R.W.G. Wyckoff, Phil. Mag, 4, 25 (1927).

9. Hand Book of Chemistry and Physics (56th edition 1975-76) Chem. Rubber Co., Press, Cleveland, Ohio, p. 200, 210.

10. V. S. Haussuhl, Z. Krist. 116, 371 (1961).

11. A. H. C. Ledsham and H. Steeple, Acta Cryst. B24, 123 (1968).

12. A. H. C. Ledsham and P. Steeple, Acta Cryst. B24, 320 (1968).

13. H. P. Klug and L. L. Liefren, J. Am. Chem. Soc. 62, 2071 (1940).

14. Ralph, W.G., Wyckoff, Crystal Structure (Ed. 2nd) Interscience Publishers (1960), A Division of John Wiley and Sons, New York.

15. H. Lipson, Phil. Mag. 19, 887 (1935).

16. A. Abragam and B. Bleaney, 'Electron Paramagnetic Resonance of Transition Ions' (Clarendon Press, Oxford 1970) p. 152.

17. J. F. Davis and M. W. P. Strandberg, Phys. Rev. 105, 447 (1957).

18. F. B. I. Goon and M. J. A. Smith, J. Phys.(Solid State) I, 2353 (1974).